



FINAL PERFORMANCE REPORT: DUAL FUEL RTU MONITORING

Prepared for: Daikin U.S. Corporation
Prepared by: Center for Energy and Environment
January 2025

CONTENTS

Summary	4
Methods	5
Power Measurements.....	5
RTU Operating Parameters	5
Weather Data	6
Airflow Measurements	6
Controls Assessment.....	6
Contractor Feedback	6
Analysis	7
Data Preparation	8
Operating Mode Determination.....	7
Performance Metrics	7
Correction Factors	8
Analysis Interval	8
Energy Savings Calculations	8
Emissions Savings Calculations	8
Results.....	9
Operating Modes.....	9
Energy Output	13
Power Input	18
Efficiency	19
Heating Loads	23
Controls Assessment.....	25
Energy Savings	26
Emissions Savings	27
Contractor Feedback	27
Timeseries Examples.....	28
Heat Pump Heating	28
Supplemental Gas Use.....	32
Appendix: Mixed Air Temperature Correction.....	38

FIGURES AND TABLES

Figure 1. Heat pump RTU instrumentation	6
Figure 2. RTU2F operating mode durations	10
Figure 3. RTU3F operating mode durations	11
Figure 4. RTU2F operating mode fraction by ambient temperature	12
Figure 5. RTU3F operating mode fraction by ambient temperature	12
Figure 6. RTU2F sensible energy transfer and temperature vs. time.....	14
Figure 7. RTU3F sensible energy transfer and temperature vs. time.....	14
Figure 8. RTU2F cumulative sensible energy transfer and temperature vs. time	15
Figure 9. RTU3F cumulative sensible energy transfer and temperature vs. time	16
Figure 10. RTU2F supply air temperature vs. outdoor temperature	17
Figure 11. RTU3F supply air temperature vs. outdoor temperature	17
Figure 12. RTU2F average power by mode and ambient temperature	18
Figure 13. RTU3F average power by mode and ambient temperature	19
Figure 14. RTU2F COP vs. temperature	20
Figure 15. RTU3F COP vs. temperature	20
Figure 16. Timeseries representation of COP calculation	21
Figure 17. RTU2F overall COP by ambient temperature bin.....	22
Figure 18. RTU3F overall COP by ambient temperature bin.....	23
Figure 19. RTU2F heating load vs. temperature.....	24
Figure 20. RTU3F heating load vs. temperature.....	24
Figure 21. RTU2F 10-minute heat pump cycles	28
Figure 22. RTU2F 20-minute heat pump cycle.....	29
Figure 23. RTU3F 40-minute heat pump cycle.....	30
Figure 24. RTU2F two-hour cycle bookended by defrosts	31
Figure 25. RTU2F 14-hour heat pump cycle.....	32
Figure 26. RTU3F gas heat cycles transitioning to heat pump heat + gas heat then heat pump heat	33
Figure 27. RTU3F heat pump heat followed by heat pump heat + gas heat then gas heating cycles	34
Figure 28. RTU3F standalone gas heat cycles.....	34
Figure 29. RTU3F gas heat cycles followed by HP heat + gas heat at lower ambient temperature	35
Figure 30. RTU3F each gas heat cycles transitions to heat pump heat + gas heat.....	35
Figure 31. RTU3F typical defrost + gas heat event	36
Figure 32. Controller on RTU2F FRONT (not monitored) showing Eff Htg Hi OAT Lk < Htg Hi OAT Lk ...	37
Figure 33. Linear Correlation of original COT – MAT to OAT – RAT in fan-only mode.....	39
Figure 34. Linear Correlation of transformed COT - MAT to OAT - RAT in fan-only mode.....	40
Figure 35. Distributions of coil outlet minus mixed air temperatures	41
Figure 36. Verification of MAT adjustment.....	42
Table 1. Datalogger fields and definitions	5
Table 2. Operating mode mapping	7
Table 3. Heating season operating mode share	13
Table 4. Distinct mode counts by RTU	25
Table 5. Quantiles of heat pump cycle duration	25
Table 6. Controls configuration persistence.....	26
Table 7. Configuration differences between RTU2F and RTU3F	26
Table 8. Energy savings calculations.....	27
Table 9. Emissions savings calculations (U.S. EPA 2024).....	27

SUMMARY

This report summarizes the performance of the 15-ton Daikin Rebel dual fuel heat pump rooftop units (RTUs) RTU2F and RTU3F serving the back zones of 47-01 Queens Blvd, Sunnyside, NY 11104 from October 19, 2023, to July 31, 2024. The performance of these heat pump RTUs was characterized in terms of operating modes, delivered sensible capacity, efficiency, energy inputs, and emissions. The information needed to calculate these characteristics was derived from high-resolution operating data transmitted by independent data loggers, configuration data from the unit controllers, and public weather databases.

During the heating season, which was defined separately for each unit as the interval between days with significant cooling demand, RTU2F operated 76.6% of the time in heat pump heating mode, 17.9% of the time in fan-only mode, 5.0% of the time in off mode, and 0.4% of the time in defrost mode. RTU3F operated 75.0% of the time in heat pump heating mode, 23.7% of the time in fan only mode, and less than 1% of the time in gas heat, defrost, heat pump heat + gas heat, defrost + gas heat, off, and heat pump cooling modes. The median heat pump cycle duration was 25.2 minutes for RTU2F and 16.5 minutes for RTU3F.

From the beginning of the monitoring period until the end of the heating season, 97% of the heating capacity of the second-floor unit was provided by the heat pump, with 3% coming from fan heat. For the third-floor unit, 94% of the heating capacity was delivered by the heat pump, 5% was fan heat, and the other 1% was provided in gas heating mode or in heat pump heat + gas heat mode.

The coefficient of performance (COP), or the ratio of heating output to RTU total energy input, was 2.59 for RTU2F and 2.53 for RTU3F over the course of the heating season. These values were calculated based on all observations. Considering only the observations classified as heat pump mode, the COP were 3.19 and 3.07 for RTU2F and RTU3F, respectively.

Compared to a conventional gas/DX RTU in the same application, these heat pump RTUs saved a significant amount of site energy and source emissions. RTU2F required 72% less site energy and RTU3F required 69% less site energy than a hypothetical conventional RTU in the same application. Heating season source emissions savings were 46% and 43% for RTU2F and RTU3F, respectively. As more electricity is sourced from zero emissions sources, the emissions savings approach the estimated heating season site emissions savings of 100% and 98% for RTU2F and RTU3F, respectively.

Contact

Grant Baumgardner
gbaumgardner@mncee.org
612-455-7857

Alex Haynor
ahaynor@mncee.org
612-244-2415

Center for Energy and Environment
612-335-5858 | www.mncee.org

METHODS

Power Measurements

A power meter (eGauge 4105) was installed at each unit to measure the power on each of the three phases feeding each RTU. The eGauge devices were connected to the internet via a cellular modem and continuously uploaded data to the eGauge server. Data at one-second intervals was retrieved from the server daily. The total electrical power input the system was calculated as the sum of the power measured on each phase.

RTU Operating Parameters

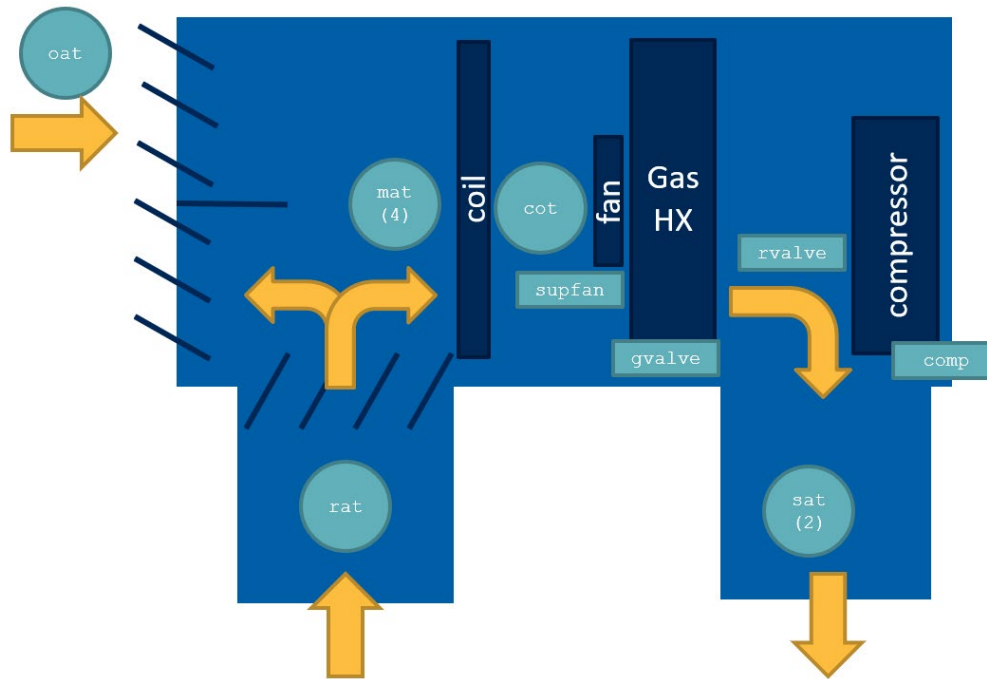
An independent data logger (Campbell Scientific CR3000) was installed at each unit to measure temperatures and actuator statuses. Temperatures were measured with field-installed thermocouples and thermocouple arrays, while heat pump RTU actuator outputs were measured with current transducers (CTs).

Table 1. Datalogger fields and definitions

Field Name	Definition	Units
datetime	timestamp	-
rec_nbr	unique ID	-
sat1	Supply Air Temperature 1	°F
sat2	Supply Air Temperature 2	°F
rat	Return Air Temperature	°F
mat1	Mixed Air Temperature 1	°F
mat2	Mixed Air Temperature 2	°F
mat3	Mixed Air Temperature 3	°F
mat4	Mixed Air Temperature 4	°F
oat	Outdoor Air Temperature	°F
cot	Coil Outlet Temperature	°F
cdt	Compressor Discharge Temperature	°F
supfan	Supply Fan Current	mV
gvalve1	Gas Valve 1 Status	mV
gvalve2	Gas Valve 2 Status	mV
rvalve	Reversing Valve Status	mV
cmp	Compressor Status	mV

Data at one-second intervals was transmitted from the logger to the storage server daily. Data was retrieved from the storage server on a weekly basis for processing and analysis. Sensor locations are shown schematically in Figure 1.

Figure 1. Heat pump RTU instrumentation



Weather Data

Weather data from the NOAA NCEI local climatological data table for La Guardia airport was downloaded on a weekly basis. Observations of outdoor temperature and relative humidity were interpolated to a one-second resolution before combining with measurements from the data logging equipment.

Airflow Measurements

Airflow was characterized through a one-time measurement and correlation approach. The initial measurements were made by inserting an array of TEC Digital TrueFlow devices into the RTU filter slot and measuring the total airflow and supply fan current at various fan speeds. A correlation curve consisting of pairs of airflow and supply fan current measurements at a total of five fan speeds ranging from 40% to 100% was used to calculate airflow based on the supply fan current, which was collected on an ongoing basis.

Controls Assessment

Over 100 status values and controls configuration parameters of interest were read from the unit controller menus and documented while on site for instrumentation installation and removal. These values were compared across visits to assess the persistence of the controls configuration and compared across units to explain differences in unit operation.

Contractor Feedback

The installing contractor for the RTUs at this site was interviewed about the differences between installing and configuring heat pump RTUs compared to traditional RTUs.

ANALYSIS

Operating Mode Determination

Next, actuator current measurements were compared with thresholds inferred from the operating data to determine whether each actuator was on (1) or off (0) at each observation. The result was recorded in a status field for each actuator. The system operating mode was inferred from the combination of statuses. In the case of defrost, the actuator statuses are identical to those of heat pump cooling, so the ambient temperature was compared to a threshold of 40°F used to classify operation as defrost or cooling.

Table 2. Operating mode mapping

Mode	Supply Fan	Compressor	Gas Valve	Reversing Valve	Ambient Temperature (°F)
Off	0	-	-	-	-
Fan Only	1	0	0	-	-
Gas Heat	1	0	1	-	-
Heat Pump Cool	1	1	0	0	> 40
Defrost	1	1	0	0	≤ 40
Heat Pump Heat	1	1	0	1	-
Defrost + Gas Heat	1	1	1	0	-
Heat Pump Heat + Gas Heat	1	1	1	1	-

Each mode was compared to its previous value to detect changes in RTU state. Data were aggregated into groups of consecutive observations where the RTU was in a consistent state for many analyses.

Performance Metrics

RTU performance metrics were calculated for each observation. Tracked metrics included supply volumetric airflow, temperature difference across the indoor coil, temperature difference across the supply fan, and temperature difference across the furnace section. These data features were combined with air properties to calculate heat pump sensible capacity, fan heating capacity, supplemental heating capacity, and net sensible heating or cooling capacity. Electric power input from the separate electric power meter was the last piece of information required to calculate the heat pump COP. The temperature difference across the heat pump indoor coil was the difference between the coil outlet temperature (COT) and the average mixed air temperature (MAT). The temperature difference across the furnace section was the difference between the supply air temperature (SAT) and the fan outlet temperature (FOT). Fan outlet temperature was estimated based on the coil outlet temperature and the theoretical

temperature rise across the fan assuming that all fan input power is converted to heat in the supply air stream. Heating capacity was the product of the volumetric airflow, physical constants, unit conversion factors, and the appropriate temperature difference. Net sensible capacity was the sum of the heat pump capacity, fan capacity, and the supplemental heating capacity.

Correction Factors

Due to the short mixing length of the RTU return air and outdoor air inlet ducts, the array of MAT sensors in this installation tended to be biased towards the outdoor air temperature (OAT). This increased the apparent COP, as the average measured MAT was lower (i.e., closer to OAT) than the physical average MAT. This was corrected by adjusting the MAT prior to the calculation of the temperature difference across the heat pump indoor coil and heat pump heating capacity. The MAT transformation assumed that the true temperature difference between the MAT and COT in fan-only mode was zero. Given the limitations of the instrumentation used, the difference between measured MAT and COT was a linear function of the difference between the OAT and return air temperature (RAT) in this application. To correct this, the final COT-MAT temperature difference and the average OAT-RAT temperature difference in every instance of fan-only mode longer than five minutes was calculated. Linear regression between these two variables revealed the coefficients of the relationship. The true MAT was then calculated as a function of the measured MAT, and a linear transformation of the OAT-RAT temperature difference. More details on this calculation approach are available in Appendix: Mixed Air Temperature Correction.

Data Preparation

The process for analyzing the data consisted of first combining the RTU data, power meter data, and weather data into a single table for each RTU. Then, out-of-range sensor values were removed and replaced with interpolated values. Values reported by sensors measuring the same physical value were averaged.

Analysis Interval

Most of the analysis focused on performance in heating season. Heating season was defined separately for each unit as operation beginning the first day following the last day of heat pump cooling in 2023 until the last day before the first day of heat pump cooling in 2024. Heating season began on October 29, 2023, for both units, and ended on May 21, 2024, and April 14, 2024, for RTU2F and RTU3F respectively.

Energy Savings Calculations

The heating season site energy savings were calculated as the difference between the actual energy input and the energy input that would be required by a hypothetical conventional RTU delivering the same net heating capacity using a gas furnace. The savings were normalized by the hypothetical energy input to estimate percent savings. In this application, the fan operated continuously, so fan energy input was equal across the actual and hypothetical scenario.

Emissions Savings Calculations

The heating season source emissions savings were calculated as the difference between the estimated source emissions and the emissions from a hypothetical conventional RTU delivering the same net heating capacity using a gas furnace. The savings were normalized by the hypothetical emissions to estimate percent savings. Emissions associated with electricity use were estimated based on measured electrical energy input multiplied by the total output emissions factor for NYCW of 0.4022 kg CO_{2e}/kWh. Emissions associated with gas use were

estimated based on an emissions factor of 53.11 kg CO₂e/mmBtu (U.S. EPA 2024). The actual gas input was estimated based on the measured supplemental heating capacity divided by the rated furnace efficiency. Site emissions savings calculations only considered the emissions associated with natural gas combustion on site.

New York City Local Law 97 (NYC LL97) includes emissions factors that are used to check compliance with the building emissions limits specified by the law. The relevant emissions factors included in NYC LL97 are 0.288962 kg CO₂e/kWh for utility electricity and 0.05311 kg CO₂e/kBtu for natural gas (New York City 2024). Note that while the natural gas emissions factor is the same as the factor assumed in this analysis, the electric emissions factor is about 28% less than the NYCW total output grid emissions factor. These NYC LL97 factors are included for reference and may optionally be used to calculate emissions savings given the information in the results section.

RESULTS

Performance was summarized in plots describing operating modes, efficiency, and delivered heating energy by energy source and ambient conditions.

Operating Modes

Operating modes were first described by a stacked bar chart with a bar corresponding to each date in the sample. The total height of the bar corresponded to the total duration of the operation observed (typically 24 hours). The color of the bar indicates the operating mode. For both units, heat pump heat mode accounted for most of the operating time during the heating season. The daily average outdoor air temperature trend overlaid on the plot shows the effect of weather on operating mode, with higher shares of heating or cooling modes when the temperature is farther away from the zone balance point temperature. For RTU2F, there were only two days with any gas use (October 22–23, 2023). For RTU3F, gas use was spread throughout the season and several occurrences of heat pump heat + gas heat and defrost + gas heating (i.e., simultaneous heat pump and gas use) were observed.

Figure 2. RTU2F operating mode durations

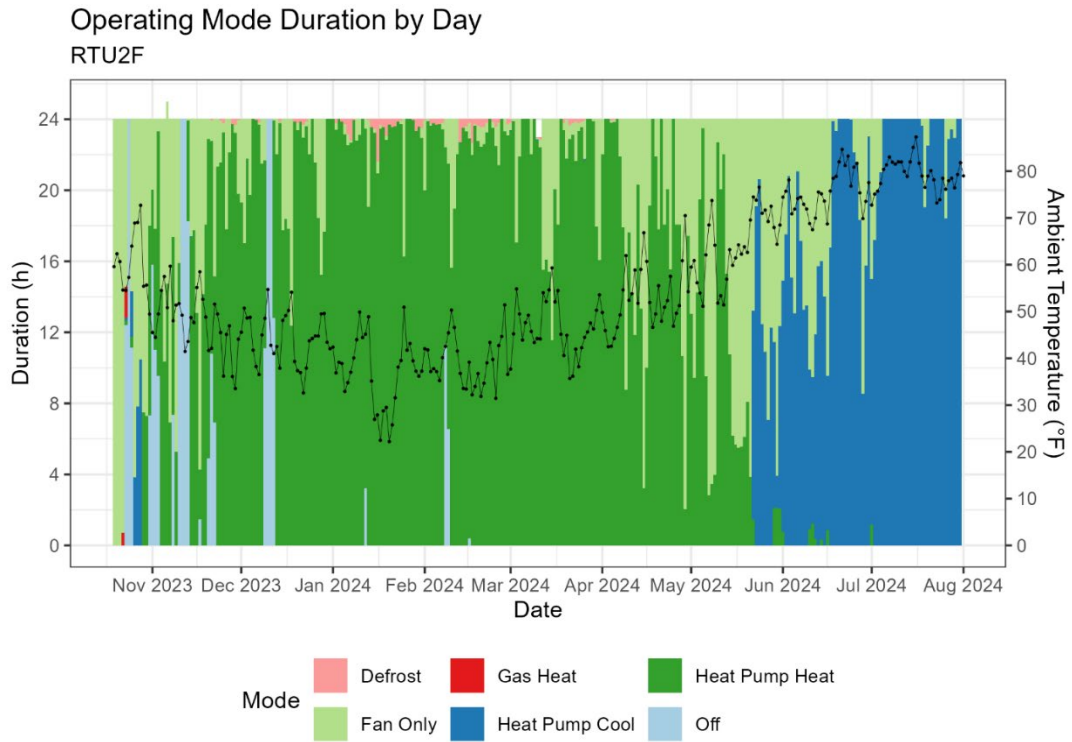
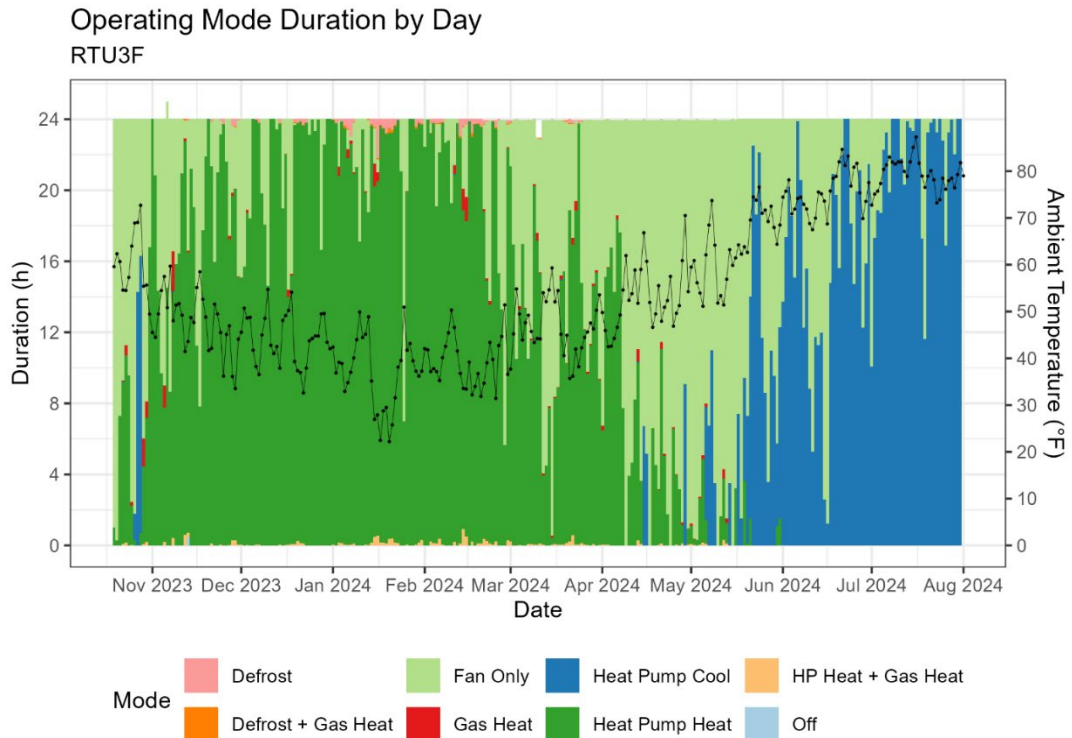


Figure 3. RTU3F operating mode durations



Operating modes were also described by a stacked bar chart showing the fraction of operating mode time by ambient temperature bin. The line overlaid on these plots indicates the total time spent in each ambient temperature bin during the study. These plots indicate the outdoor temperatures where the RTUs transition between heating, ventilation, and cooling in this application. They also show that defrost is a larger share of operation in the (25°F, 30°F] bin than any other.

Figure 4. RTU2F operating mode fraction by ambient temperature

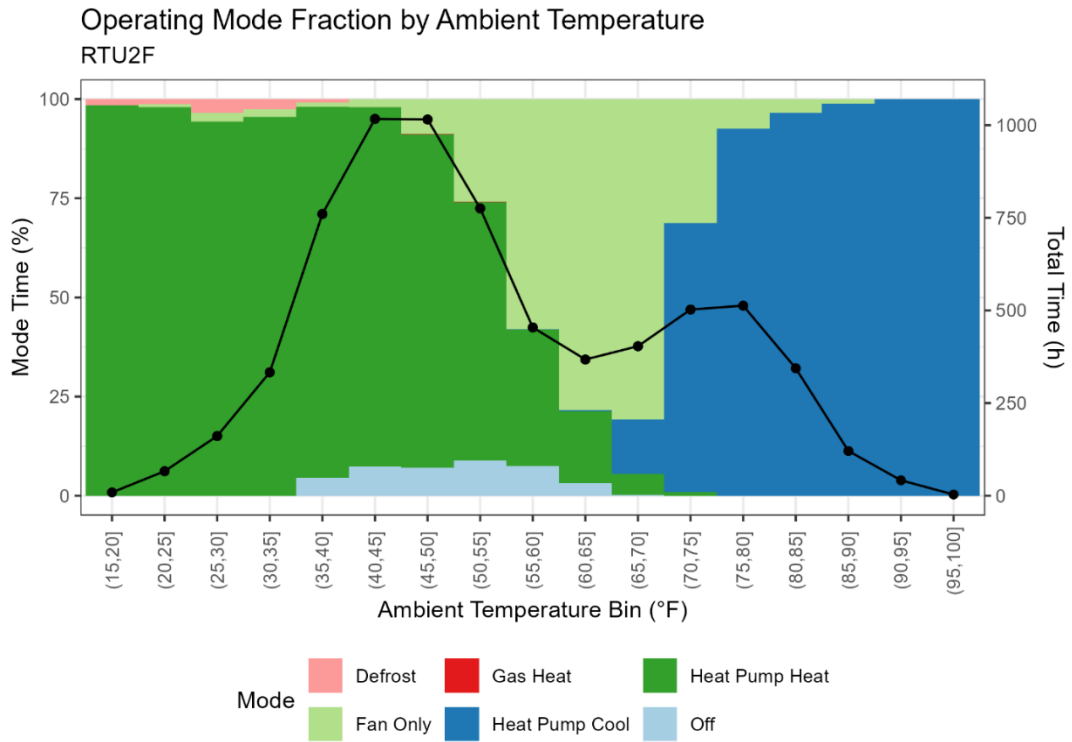
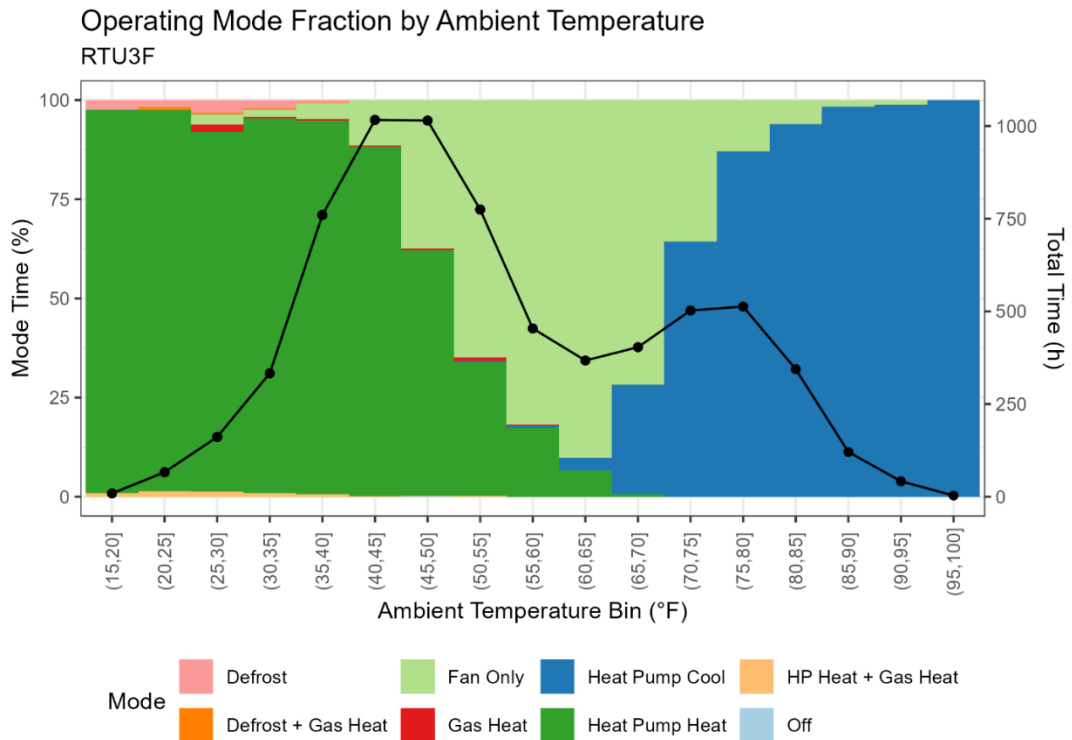


Figure 5. RTU3F operating mode fraction by ambient temperature



Overall mode fractions during the heating season for each unit are shown in Table 3. Only heat pump heat, fan-only, and off mode make up more than 0.5% of the operating time for either RTU.

Table 3. Heating season operating mode share

Mode	RTU2F Operating Time	RTU3F Operating Time
Defrost	0.46 %	0.46%
Heat Pump Heat + Gas Heat	-	0.36%
Defrost + Gas Heat	-	0.08%
Fan-only	17.92%	23.66%
Gas Heat	-	0.46%
Heat Pump Cool	0.00%	0.01%
Heat Pump Heat	76.57%	74.97%
Off	5.05%	0.01%

Energy Output

The delivered energy plot shows another timeseries view with a bar corresponding to each date. The height of the bar corresponds to the sensible heating or cooling energy delivered, while the color represents the operating mode. These plots were used to define the heating season for both units, highlighting the last day of cooling in 2023 and first day of cooling in 2024. This plot also includes a line plot overlay that shows the daily average temperature on the right y-axis. Higher outdoor air temperatures are coincident with lower delivered heating energy and vice versa. The heating capacity of the supply fan is not negligible and appears to play a significant role in providing heat during the end of the heating season. On the coldest days, approximately 5% to 10% of the heating capacity delivered is used to cancel out the cooling effect of defrost. Supplemental heat use in RTU3F provides very little heating capacity and appears to be uncorrelated to temperature.

Figure 6. RTU2F sensible energy transfer and temperature vs. time

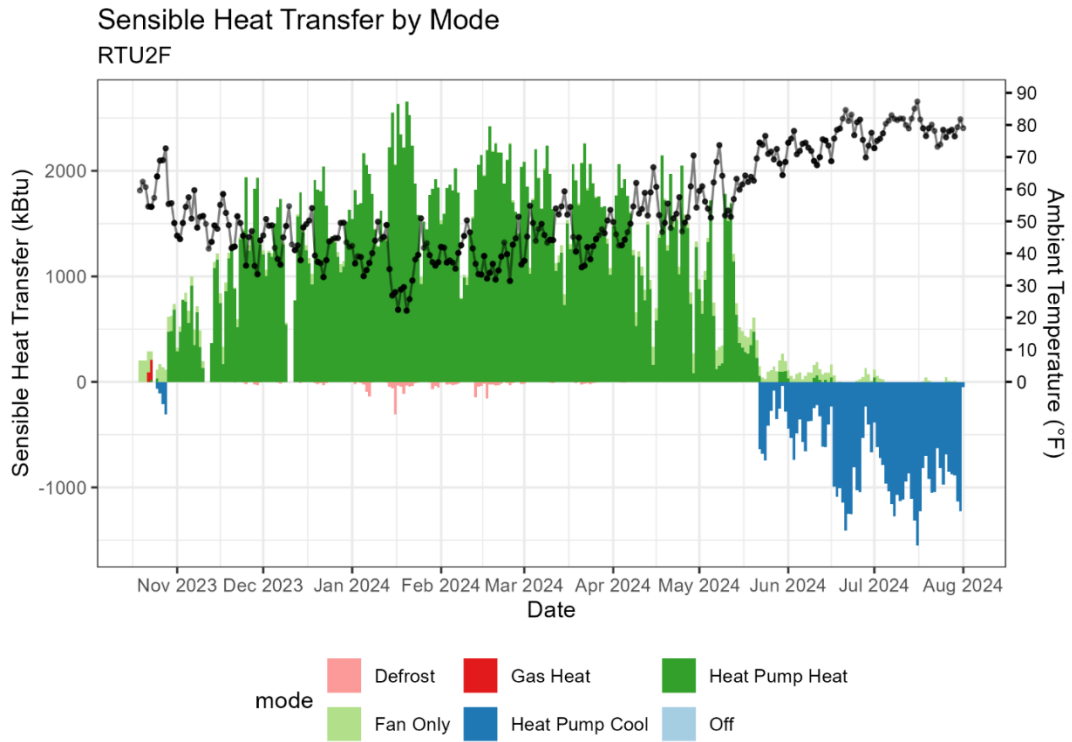
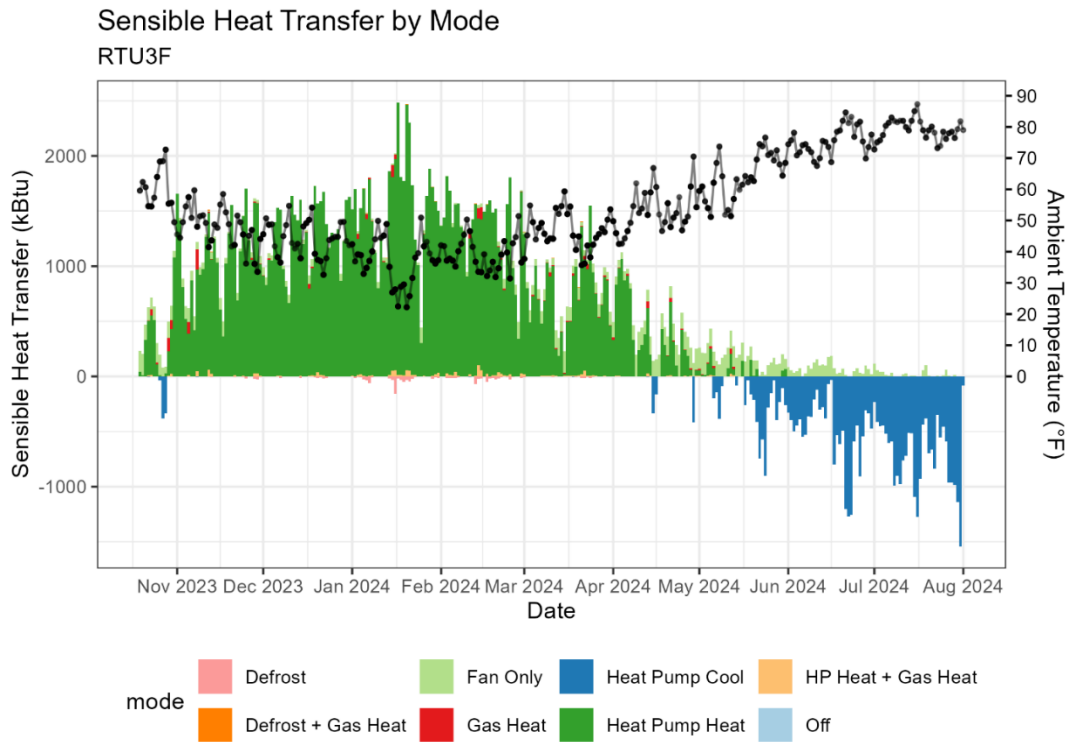


Figure 7. RTU3F sensible energy transfer and temperature vs. time



Cumulative Energy Output

The cumulative version of the sensible heat transfer plots reveal additional insights into the overall RTU performance. The plots are very similar for both RTUs, with the vast majority of energy output throughout the monitoring period corresponding to heat pump heating. The negative capacity associated with defrost is very small. As the weather warms in the spring, heat pump heating begins to taper off and more energy transfer is associated with fan-only mode. By the time heat pump cooling energy transfer begins, heat pump heating has leveled off for the year. For RTU3F, the net capacity delivered in any of the modes using gas (gas heat, heat pump heat + gas heat, and defrost + gas heat) is very small relative to heat pump heating. Over the monitoring period, RTU2F output roughly 300 MMBtu of energy to the zone and extracted roughly 50 MMBtu of energy from the zone. RTU3F output about 225 MMBtu to the zone it served and extracted almost 50 MMBtu.

Figure 8. RTU2F cumulative sensible energy transfer and temperature vs. time

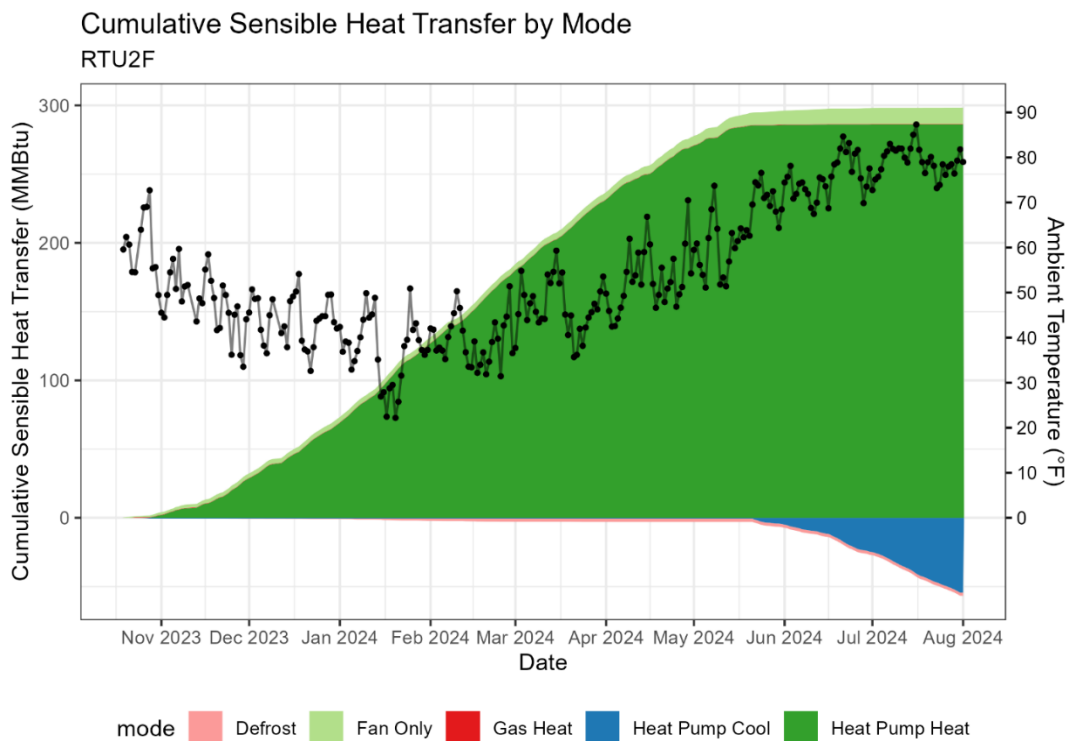
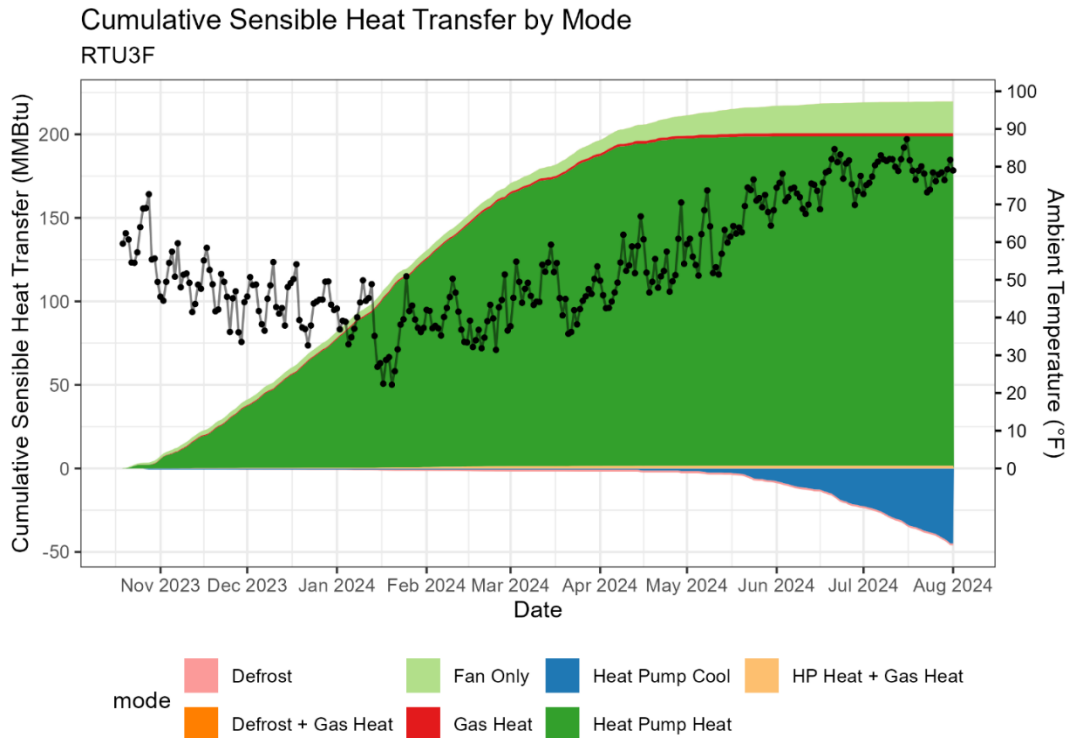


Figure 9. RTU3F cumulative sensible energy transfer and temperature vs. time



Supply Air Temperature

Supply air temperature during heat pump heating was plotted against outdoor air temperature to verify that the supply air temperature was maintained at sufficiently high levels as the outdoor temperature decreased. The y-value of each point represents the average supply air temperature, and the point color corresponds to the average input power during the heat pump heating cycle. Higher compressor power corresponds to higher compressor speed. The results showcase the benefit of variable speed heat pumps, which were able to maintain a range of comfortable supply air temperatures across a wide range of ambient conditions by modulating the compressor speed.

Figure 10. RTU2F supply air temperature vs. outdoor temperature

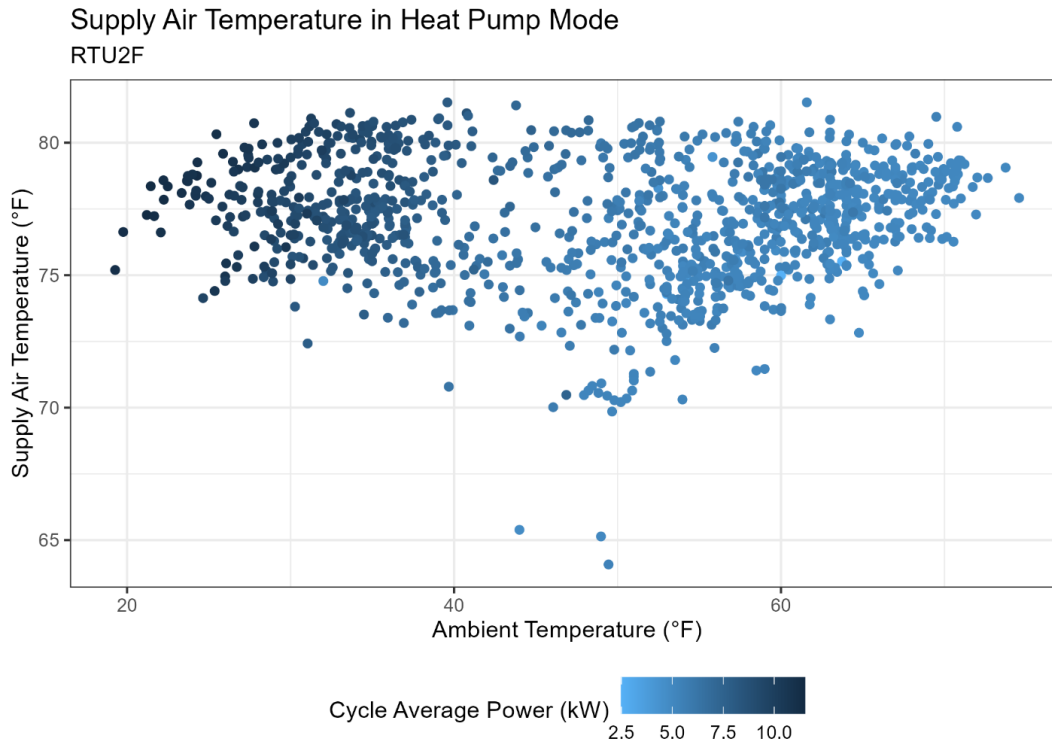
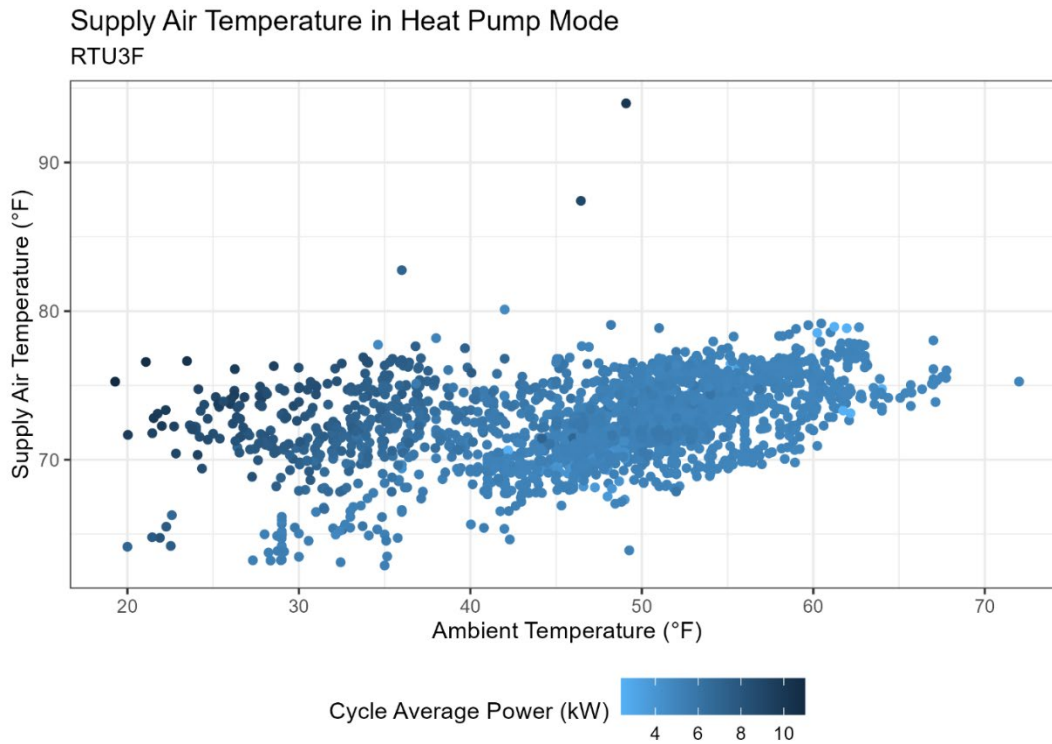


Figure 11. RTU3F supply air temperature vs. outdoor temperature



Power Input

Electric power input was characterized by plotting the average power by mode and ambient temperature bin. The size of the point maps to the total amount of operation in the corresponding conditions. There were three distinct power levels corresponding to the status of the compressor and supply fan. Off mode has near-zero power input, fan-only mode has a relatively constant power input of about 2.5 kW, and heat pump modes varied in power requirements from about 5 kW at moderate ambient temperatures up to 12 kW for peak heating and beyond 15 kW for peak cooling. Defrost required a relatively constant power input around 6 kW that decreased with decreasing ambient temperature. Gas furnace operation required only a small increase in electric power input.

Figure 12. RTU2F average power by mode and ambient temperature

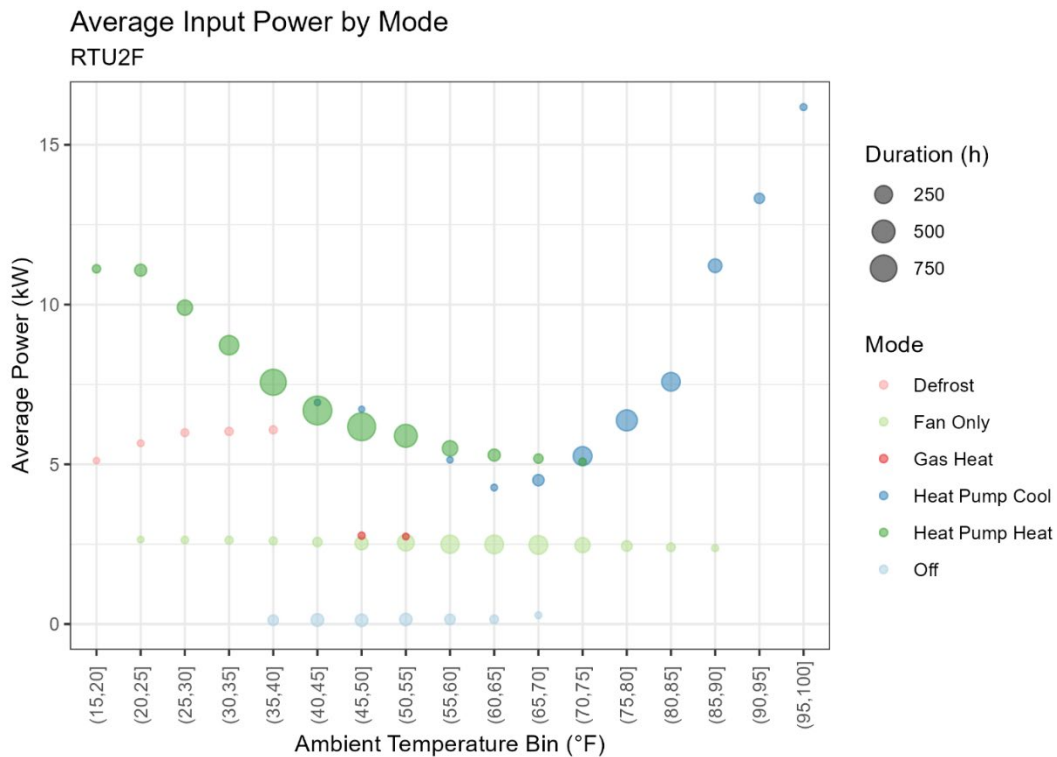
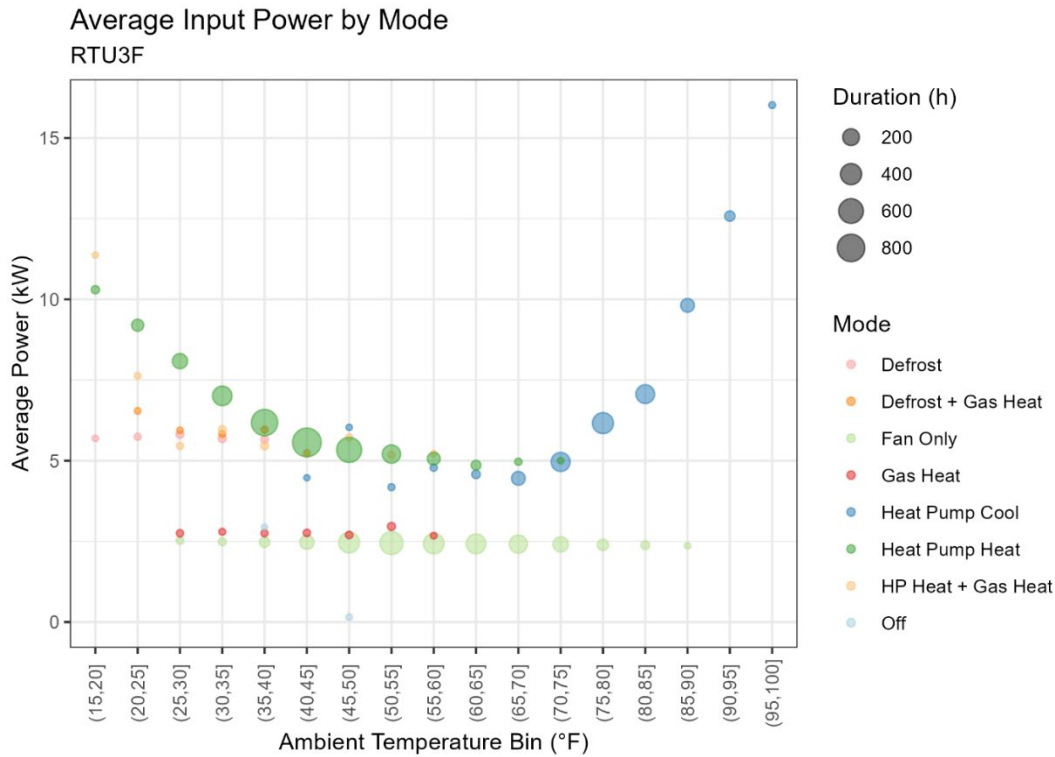


Figure 13. RTU3F average power by mode and ambient temperature



Efficiency

Efficiency was first described in plots of COP vs. ambient temperature. Each point represented one period of compressor operation in heat pump heating mode, or one heating cycle. The size of the point corresponded to the duration of the cycle, while the X and Y location indicate the average ambient temperature and average COP during the cycle, respectively.

These plots show that RTU3F cycled the compressor more often than RTU2F (n = 2169 vs n = 1136) over their heating seasons. Charts for both units showed COP maximized with respect to ambient temperature around 47°F outdoor temperature. At the coldest observed cycle average temperatures of around 20°F, both units still provided heating at COPs around 3.

Figure 14. RTU2F COP vs. temperature

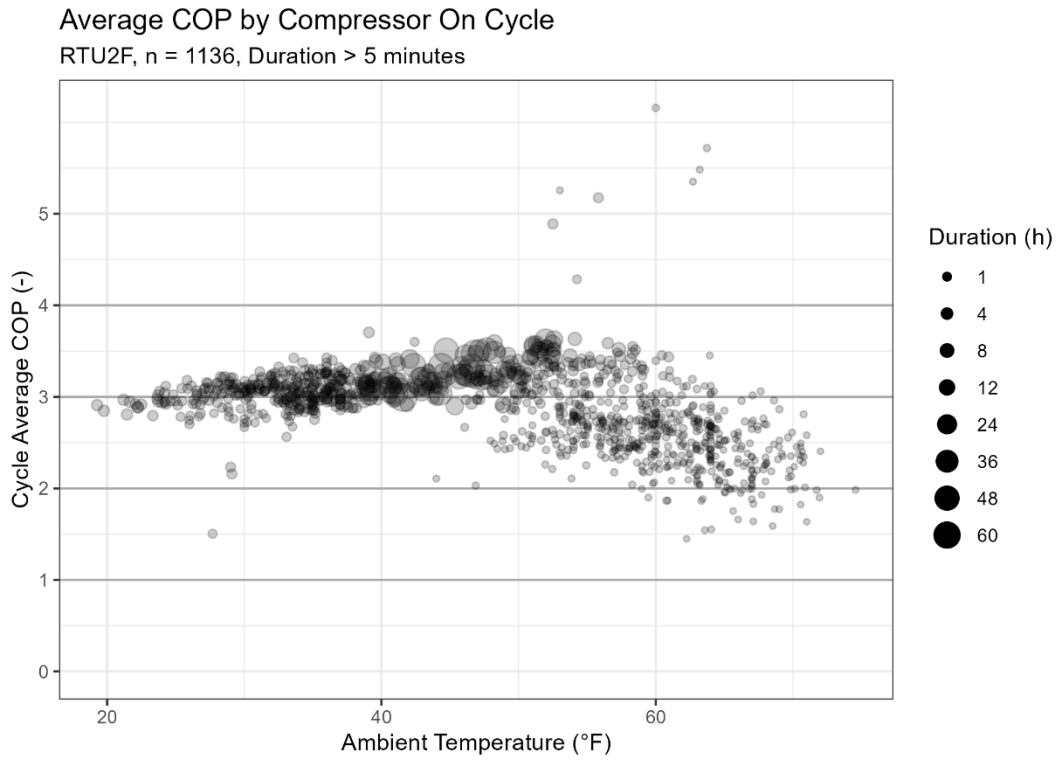
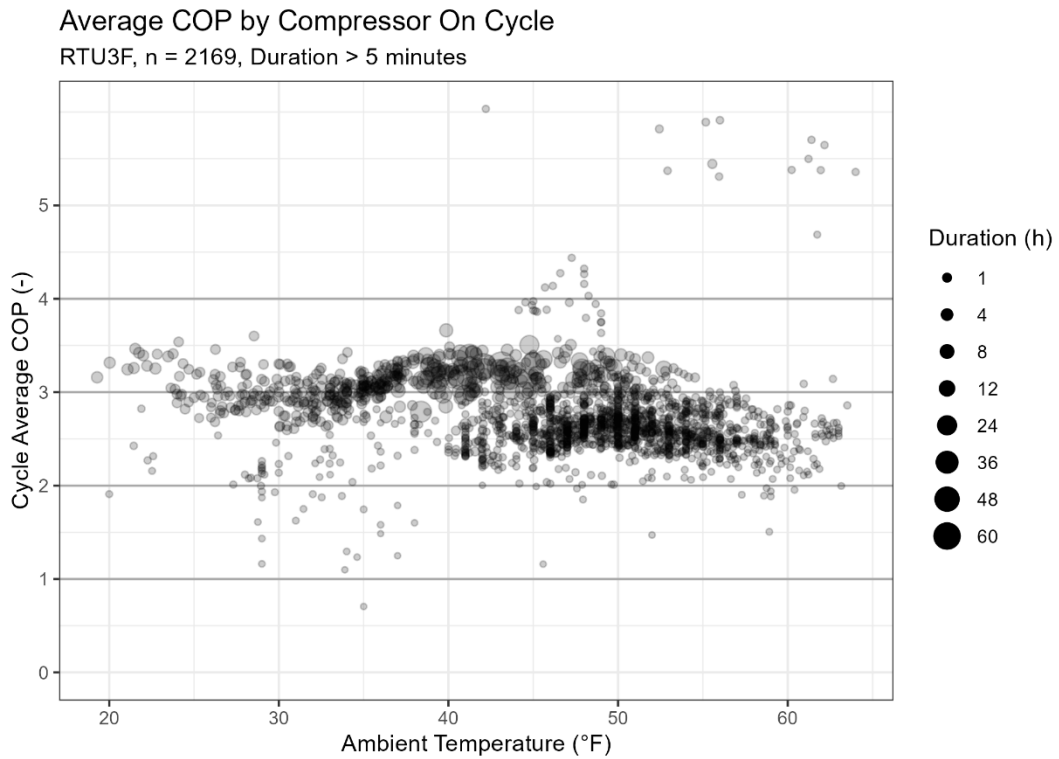
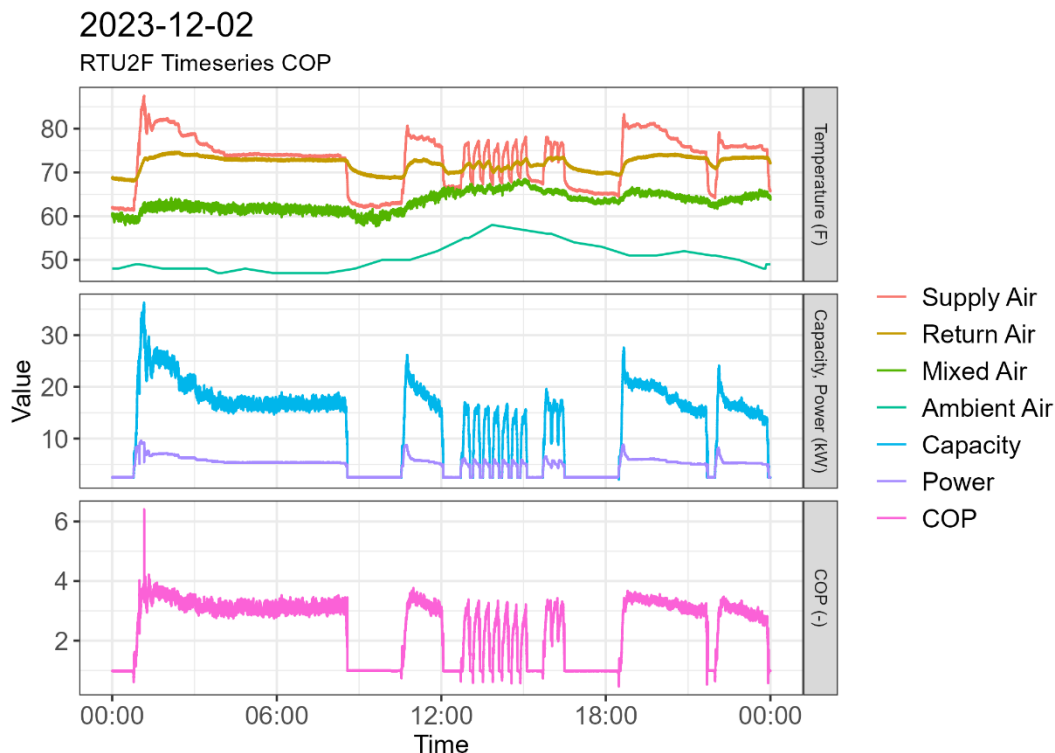


Figure 15. RTU3F COP vs. temperature



The duration of the heating cycle had a large impact on the average COP because the instantaneous COP changed significantly within a given cycle. Typically, the instantaneous COP value, calculated as the ratio of the capacity output to power input, increased from a value around 1 at the beginning of the cycle towards a steady-state value around 3 after about 15 minutes when the full heating capacity of the system developed. Cycles began with a COP around 1 because in this application, heating modes were entered from fan-only mode, where the ratio of heating capacity from the supply fan and power input to the supply fan was assumed to be 1. This transient ramp up in COP from 1 to the steady-state value was a relatively large portion of the shortest cycles and brought down the cycle average COP, while the transient portion's impact on the cycle average COP of longer cycles was negligible. Cycle length was shorter at lower ambient temperatures because regular defrosts were required to maintain heating capacity. Cycle duration was shorter at higher ambient temperatures because the heating load was lower than the minimum capacity the units could supply in steady-state operation, so the units cycled off to avoid overheating the space. Figure 16 shows how the COP develops throughout a heating cycle for cycles of different lengths. The longer morning cycle reaches a steady value around 3 and continues to operate at that condition for several hours. The shorter cycles in the warmer part of the day from 12:00 to 15:00 never reach steady-state, and the average COP of those cycles is closer to 2.5.

Figure 16. Timeseries representation of COP calculation



Another view of efficiency shows the overall COP (across all modes) by outdoor temperature bin throughout the heating season. Note that heating season lasts longer into 2024 for RTU2F so there is data at higher ambient temperatures. When taken together with the plots of operating mode fraction by ambient temperature bin, the impact of defrost on COP emerges, as the (25, 30]°F bin has a lower COP than neighboring bins for both RTUs. The COP approached 1.00 at higher ambient temperatures because these bins mostly consisted of fan-only operation, where 100% of input power was converted to heat in the airstream. Across all modes and ambient

conditions, RTU2F achieved a heating season COP of 2.98 and RTU3F achieved a COP of 2.71.

Figure 17. RTU2F overall COP by ambient temperature bin

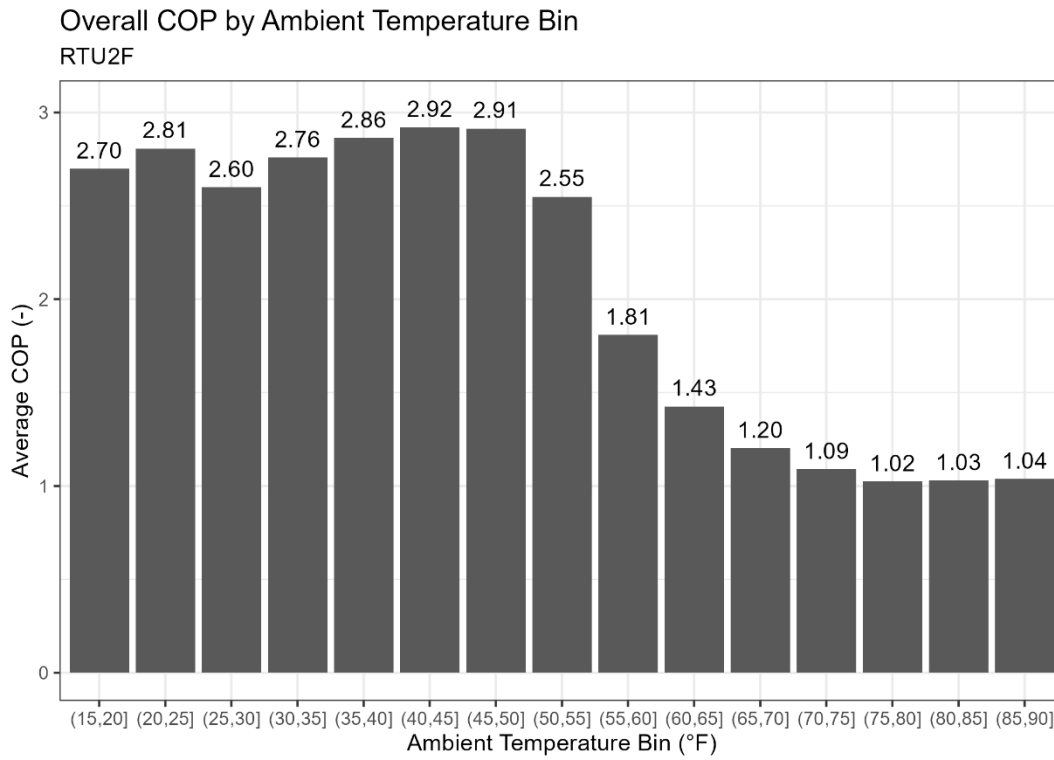
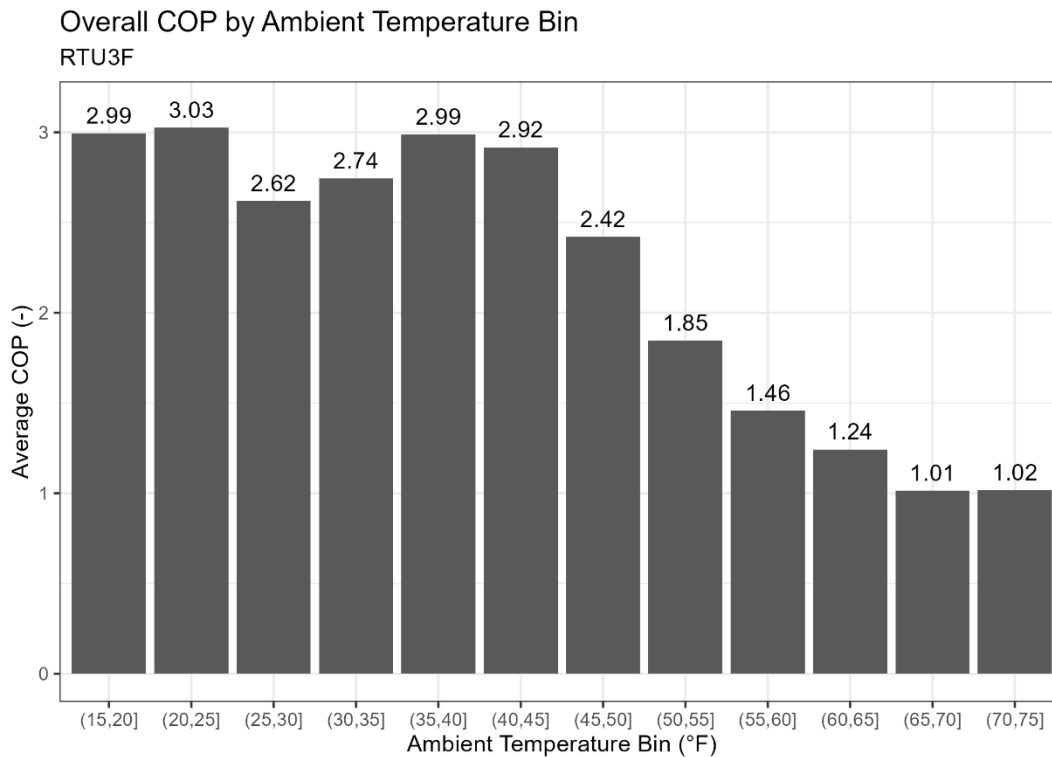


Figure 18. RTU3F overall COP by ambient temperature bin



Heating Loads

Calculating the heating energy delivered by the heat pumps facilitated the empirical calculation of the zone heating load, assuming that the equipment was able to meet the space setpoint throughout the heating season. The daily average heating capacity delivered is shown with respect to the daily average temperature in a scatterplot. The daily average heating capacity is based on the net heating capacity, summing the effects of the heat pump coil, supply fan, and supplemental heat system. This scatterplot shows an inverse correlation during heating season, as the required heating capacity decreases with increasing temperature. Design documents for this retrofit indicated that the load at the design temperature of 17°F was 98,356 Btu/h for the zone served by RTU2F and 102,130 Btu/h for the zone served by RTU3F.

The empirical zone heating load was 121,111 Btu/h for RTU2F and 105,113 Btu/h for RTU3F. With a rated heat pump heating capacity of 91,000 Btu/h at 17°F, supplemental heating was expected to be necessary when daily average temperatures approached 17°F. The coldest observed temperature in the winter of 2023–2024 was 19°F, and supplemental heating was apparently not used to maintain the space temperature.

Figure 19. RTU2F heating load vs. temperature

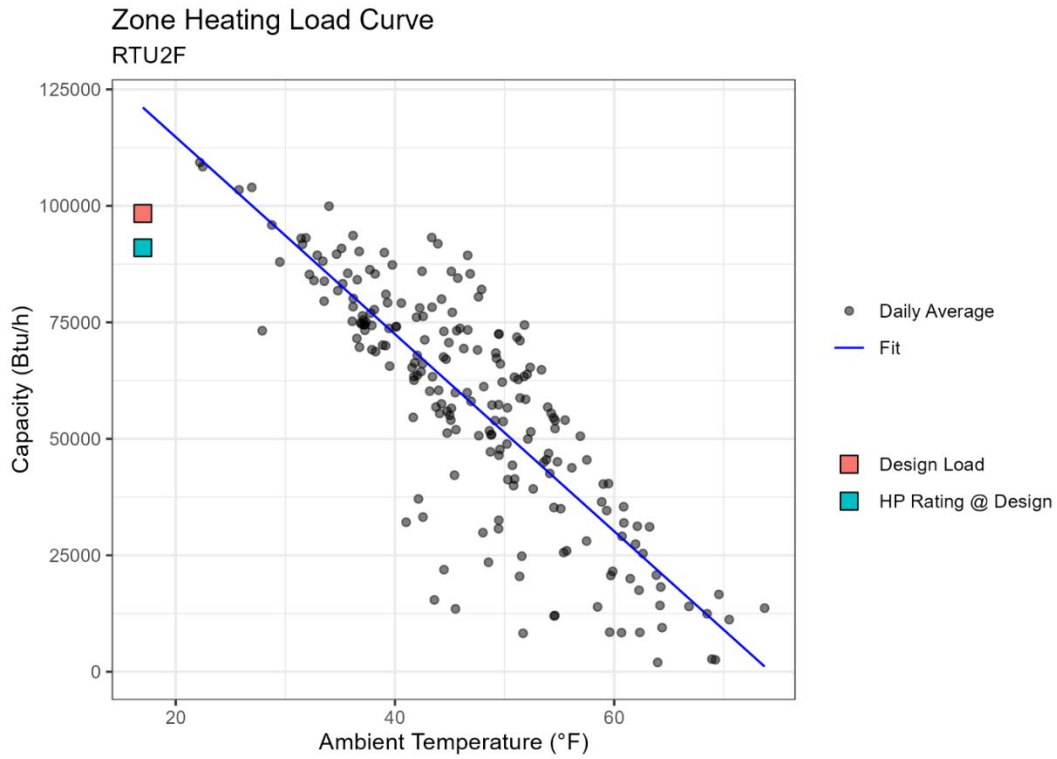
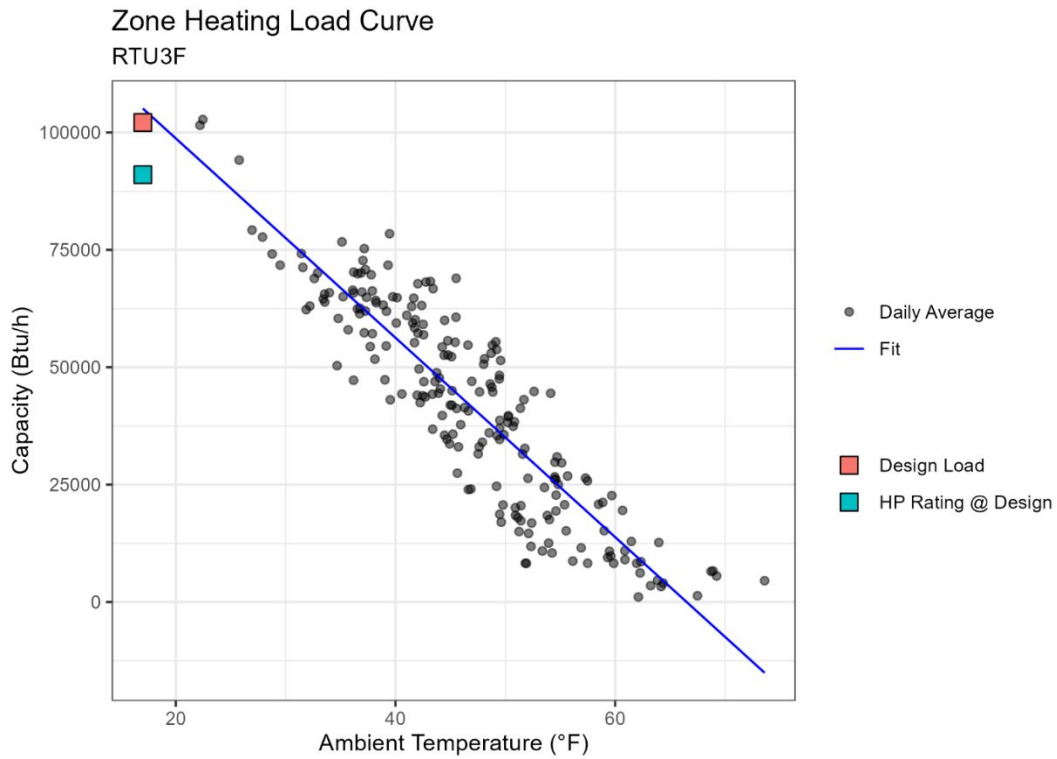


Figure 20. RTU3F heating load vs. temperature



Controls Assessment

Operating Mode Counts

Throughout the monitoring period (October 19, 2023, to July 31, 2024) the RTUs changed state in response to control logic and sensor input. The distinct count of each mode by RTU is shown in Table 4.

Table 4. Distinct mode counts by RTU

Mode	RTU2F Count	RTU3F Count
Off	35	3
Fan Only	2934	4553
Gas Heat	18	400
Heat Pump Cool	1468	1645
Defrost	388	361
Heat Pump Heat	1385	2448
Defrost + Gas Heat	0	107
Heat Pump Heat + Gas Heat	0	330

Typical Heating Cycle Duration

The RTUs exhibit a mix of long and short heat pump heating cycles. Table 5 shows selected quantiles of heat pump cycle duration for each RTU. Shorter cycles are on the order of about 10 minutes, while longer cycles may last for hours. The duration of the longest cycles was significantly longer for RTU2F.

Table 5. Quantiles of heat pump cycle duration

Cycle Duration Percentile	RTU2F	RTU3F
5%	4.43 minutes	8.82 minutes
25%	11.8 minutes	13.7 minutes
50%	25.2 minutes	16.5 minutes
75%	2.01 hours	40.0 minutes
95%	14.3 hours	4.38 hours

Controls Configuration Persistence

For each unit, most of the changes between configuration documented during the visit in January 2024 and the final site visit in September 2024 were setpoint changes. The occupied cooling and heating setpoints and the discharge air temperature (DAT) cooling and heating setpoints changed for both units. In addition, the control temperature source was updated on RTU2F.

Table 6. Controls configuration persistence

Parameter	RTU	Value 01/12/2024	Value 09/30/2024	Default Value
Occ Clg Spt (°F)	2F	74	71	72
Occ Htg Spt (°F)	2F	74	70	68
DAT Clg Spt (°F)	2F	68.6	71	55
DAT Htg Spt (°F)	2F	74	71.8	85
Ctrl Temp Src (°F)	2F	Space	RAT	RAT
Occ Clg Spt (°F)	3F	75	70	72
Occ Htg Spt (°F)	3F	73	70	68
DAT Clg Spt (°F)	3F	59.7	70	55
DAT Htg Spt (°F)	3F	69.6	71.9	85

Controls Configuration Differences Between RTUs

Aside from temperature setpoints, the configuration differences between RTU2F and RTU3F were few but significant in terms of their impact on supplemental heating use. The key configuration difference between the two units was the **Spl Htg OAT Lk** setting. This setting, which prevents supplemental heating use above the configured value, was left at its default value of 55°F for RTU3F, while it was changed to 0°F for RTU2F. **Htg Stg Time**, the minimum time between heating stage changes, was changed from its default on RTU2F. This could explain why the shortest heating cycles for RTU2F were shorter than those for RTU3F. The **DuctSP Spt** sets the duct static pressure set point used for controlling the speed of the supply air fan. However, both units were configured to use a constant fan speed, so this value had no impact on the operation of the units. The **Htg Hi OAT Lk** is a high outdoor ambient temperature value above which compressor heating is locked out. This was apparently changed to allow compressor heating above the default value of 55°F. Heat pump heating was observed up to the (70, 75] °F ambient temperature bin for both units. The **Max Htg Spt** setting sets the maximum heating discharge set point for use with a heating discharge air temperature set point reset schedule (Daikin Applied 2023).

Table 7. Configuration differences between RTU2F and RTU3F

Parameter	RTU2F Value 01/12/2024	RTU3F Value 01/12/2024	Default Value
DuctSP Spt (in H ₂ O)	0.1	1	1 in H ₂ O
Htg Stg Time (min)	2	5	5 min
Htg Hi OAT Lk (°F)	90	100	55
Spl Htg OAT Lk (°F)	0	55	55
Max Htg Spt (°F)	80	75	120

Energy Savings

RTU2F required 72% less site energy and RTU3F required 69% less site energy than a hypothetical conventional RTU in the same application. The inputs of the energy savings calculation are given in Table 8. These calculations assume that the fan would operate the same way in the hypothetical gas-fired RTU scenario as it did for the observed heating season, so the fan energy input and output is assumed to be the same as observed and the hypothetical heating energy input required is based only on the heat actually delivered by the heat pump and gas furnace sections.

Table 8. Energy savings calculations

ID	Parameter	Calculation	RTU2F	RTU3F
A	Actual Energy Input(kWh)	[measured]	28,593	21,711
B	HP & Gas Heat Delivered (kBtu)	[measured]	250,961	167,228
C	Furnace Efficiency	[unit data]	0.81	0.81
D	Hypothetical Gas Input (kBtu)	B / C	309,828	206,455
E	Median Fan Power (kW)	[measured]	2.48	2.42
F	Heating Season Time (h)	[measured]	4,695	4,053
G	Fan Energy Input (kWh)	E * F	11,652	9,824
H	kWh/kBtu	[conversion]	0.293	0.293
I	Total Hypothetical Energy (kWh)	(D * H) + G	102,432	70,315
J	Savings (%)	$100 * (I - A) / I$	72.1	69.1

Emissions Savings

Heating season source emissions savings were 46% and 43% for RTU2F and RTU3F, respectively. If more electricity comes from zero emissions sources in the future, the emissions savings will approach the estimated heating season site emissions savings of 100% and 98% for RTU2F and RTU3F, respectively.

Using NYC LL97 emissions factors (0.288962 kg CO₂e/kWh electric emissions factor, same gas emissions factor) gives actual emissions of 8,262 kg CO₂e and 6,170 kg CO₂e, and emissions savings of 58% and 55% relative to a conventional RTU in the same application for RTU2F and RTU3F respectively.

Table 9. Emissions savings calculations (U.S. EPA 2024)

ID	Parameter	Calculation	RTU2F	RTU3F
A	Electric Emissions Factor (kg CO ₂ e /kWh)	[conversion]	0.4022	0.4022
B	Gas Emissions Factor (kg CO ₂ e /kBtu)	[conversion]	0.05311	0.05311
C	Actual Electric Input (kWh)	[measured]	28,593	20,749
D	Actual Gas Input (kBtu)	[estimated]	0	3,285
E	Actual Emissions (kg CO ₂ e)	A * C + B * D	11,500	8,520
F	Hypothetical Electricity Input (kWh)	[Table 8: G]	11,652	9,824
G	Hypothetical Gas Input (kBtu)	[Table 8: D]	309,828	206,455
H	Hypothetical Emissions (kg CO ₂ e)	A * F + B * G	21,141	14,916
I	Emissions Savings (%)	$100 * (H - E) / H$	46%	43%

Contractor Feedback

The installing contractor reported that there was no difference in installation between heat pump and conventional RTUs. The only hardware differences noted were additional sensors and controls on the heat pump units, but because those were factory installed, they were not important from the installer perspective. Regarding control configuration, the contractor reported that setup was quite easy, and there were no extra setup or startup steps beyond what was done for conventional RTUs. When asked about supplemental heating use, the contractor

reported that the heat pumps were very efficient at heating, and the gas heating was not expected to kick on. The contractor had never observed supplemental heating use during service visits.

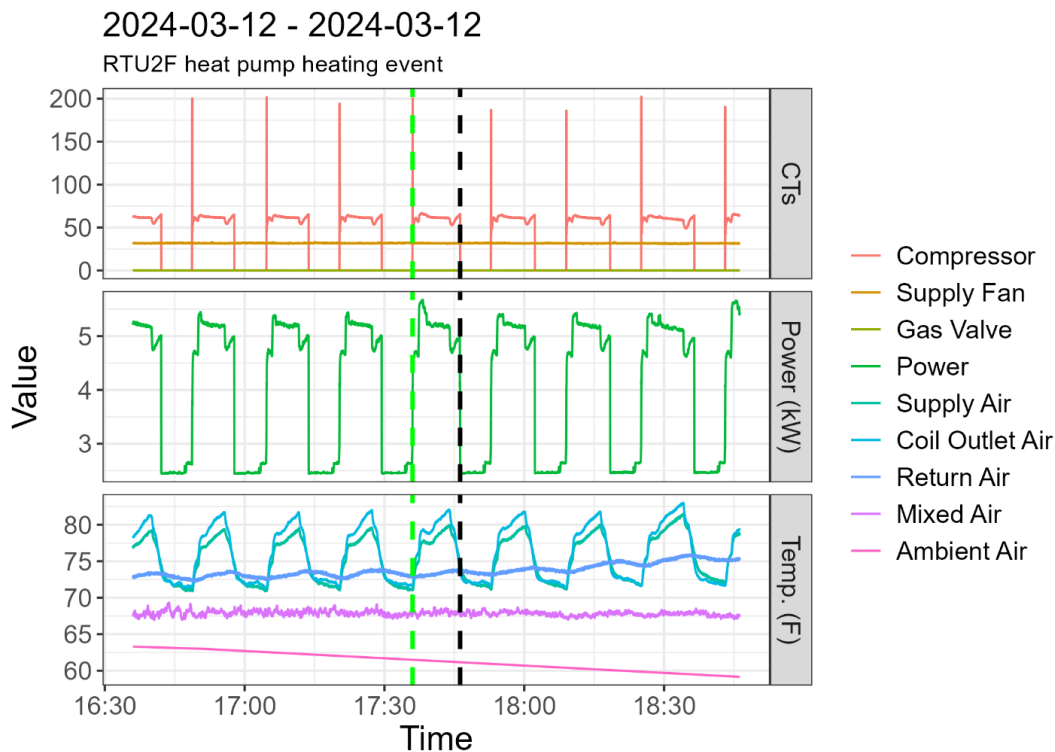
TIMESERIES EXAMPLES

The aggregated data followed expected trends, showing that the dominant operating mode during the heating season was heat pump heating, COP matched its rated values, and the empirical and theoretical zone heating load closely matched. The following plots show the underlying data to provide additional context and support for the results. Each plot shows an hour of operation on either side of a single operating mode. The vertical green dashed line indicates the beginning of the cycle of interest, and the vertical black dashed line indicates the end.

Heat Pump Heating

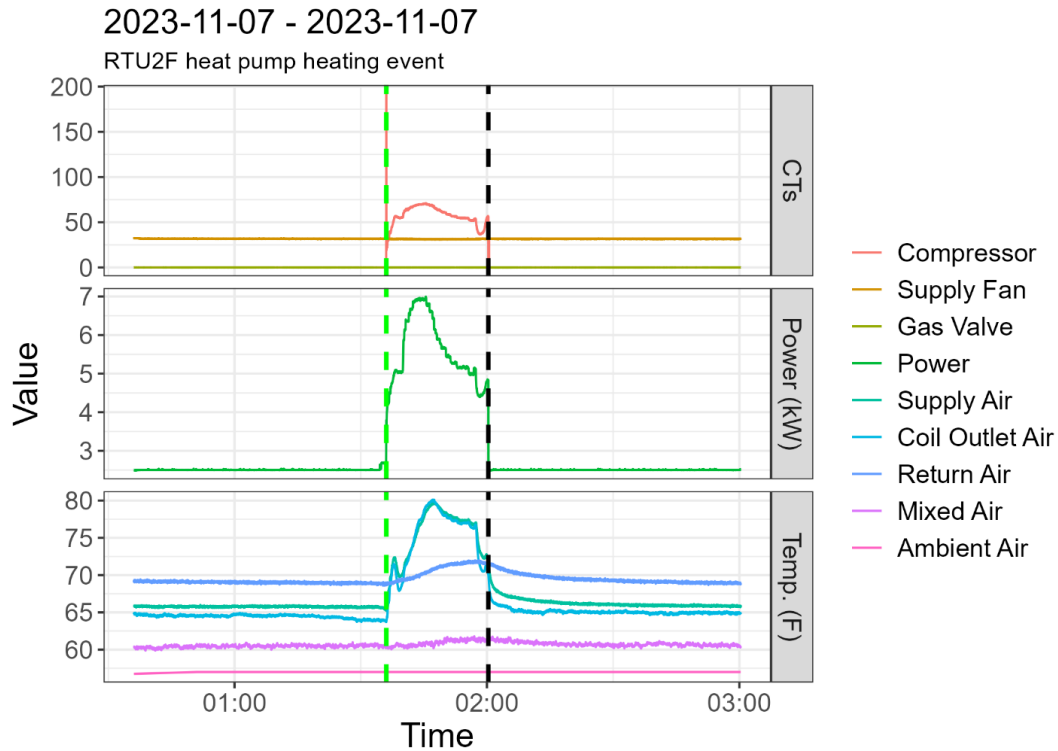
The first plot shows an approximately 10-minute heat pump cycle that is surrounded before and after by many similar cycles. This behavior was typical in warmer ambient conditions like these. With only a small amount of heating capacity required at 60°F ambient, the heat pump is unable to modulate capacity low enough to run continuously.

Figure 21. RTU2F 10-minute heat pump cycles



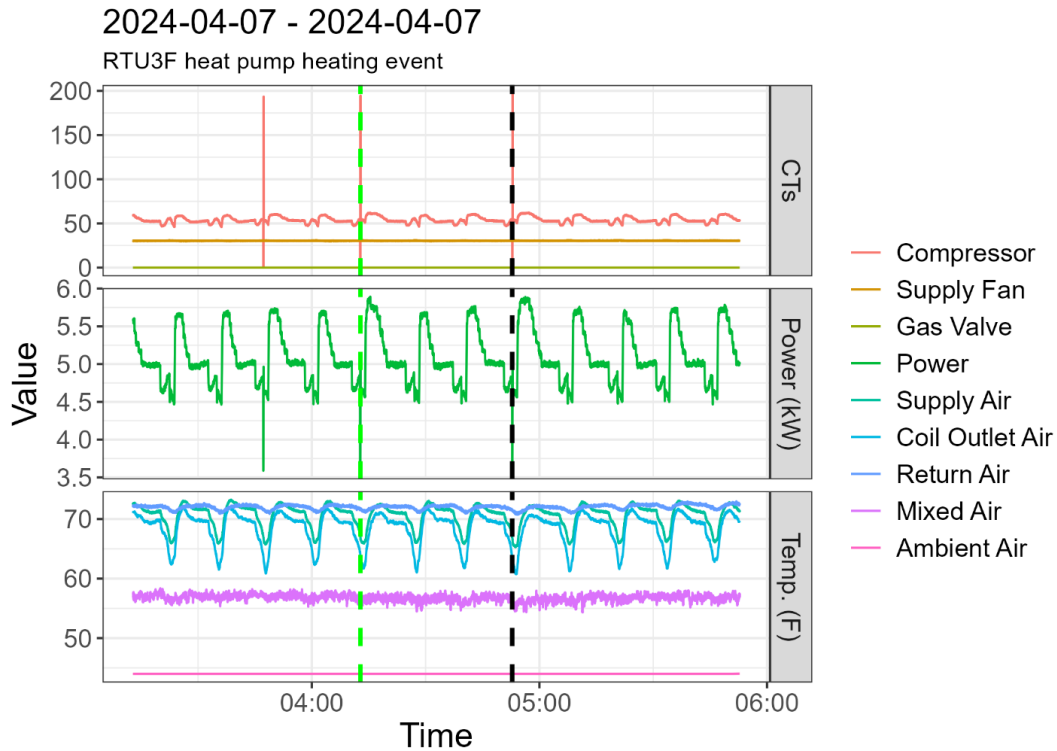
Sometimes, heat pump cycles were more isolated. The 20-minute heat pump cycle shown in Figure 22 occurs shortly after midnight. No heat pump cycles within an hour on either side were observed.

Figure 22. RTU2F 20-minute heat pump cycle



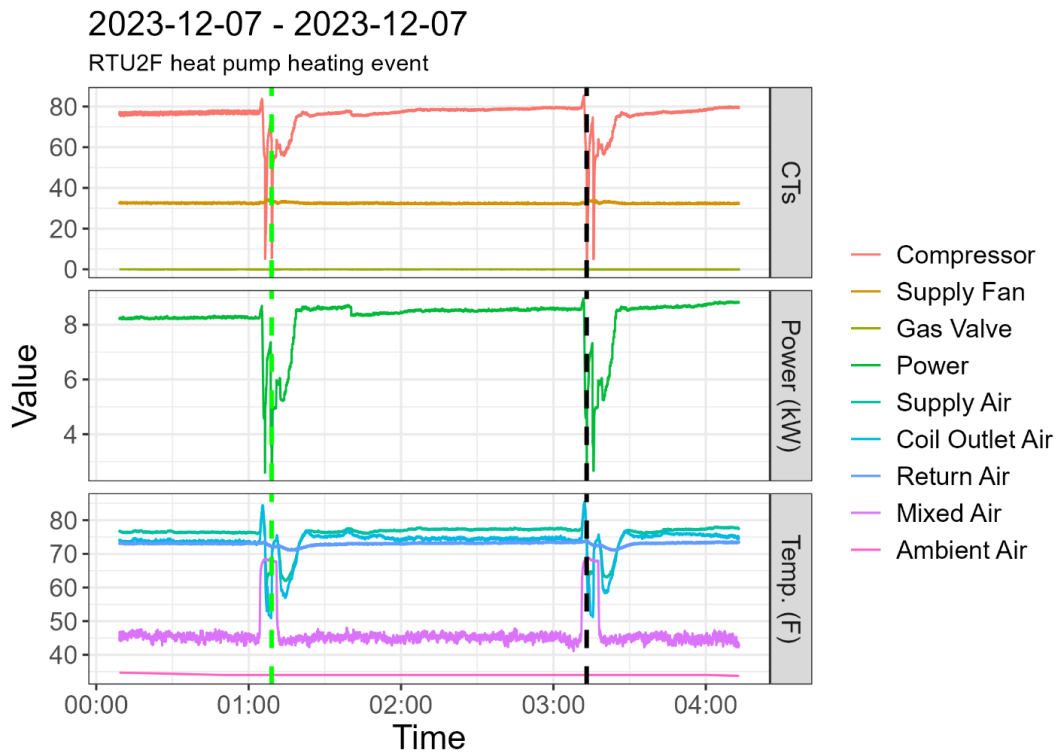
The median cycle duration for RTU3F was about 40 minutes. Figure 23 shows a typical median-length cycle for RTU3F. The system appears to be repeatedly modulating capacity up and down and only occasionally shuts off the compressor, as seen in both the “Compressor” and “Power” signals. This behavior was observed less frequently on RTU2F which is likely why RTU3F has shorter cycles and more cycles overall. It was unclear whether this behavior was driven by temperature control requirements or other functions of the unit controller.

Figure 23. RTU3F 40-minute heat pump cycle



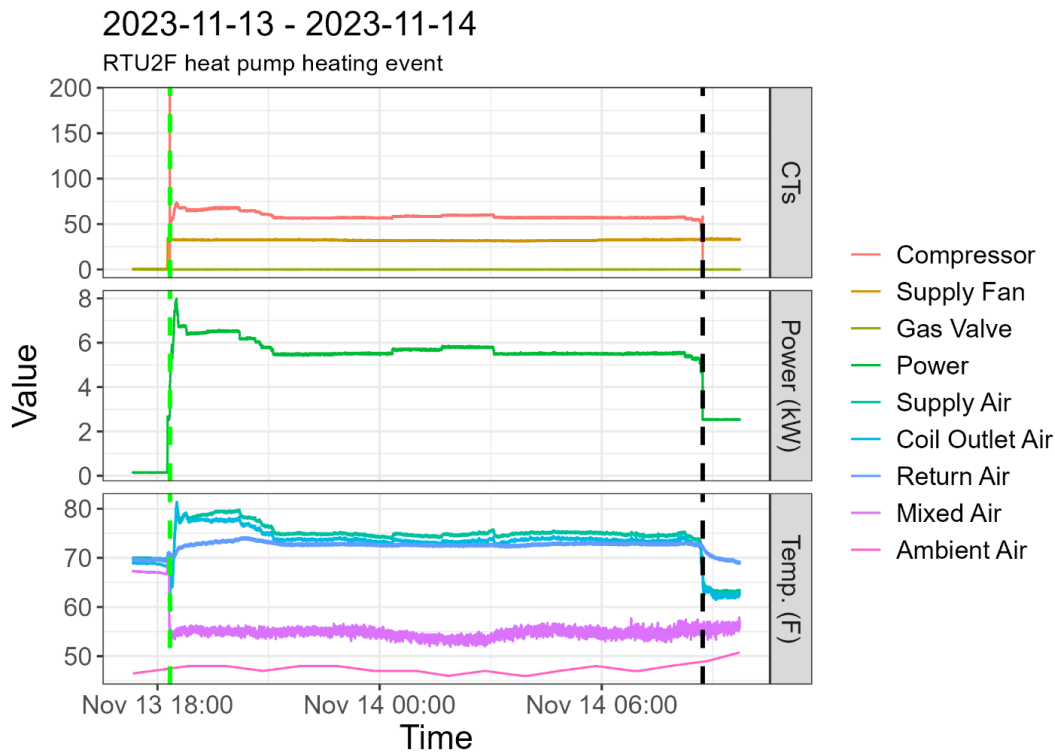
The two-hour heat pump cycle from RTU2F shown in Figure 24 starts and ends with a defrost event. Previous analysis showed that defrosts were more common with ambient temperatures around 30°F, as they are in this example. With many RTU2F cycles about two hours in duration, the unit controller was likely using a timer to trigger defrosts, at least in ambient conditions that were likely to require them.

Figure 24. RTU2F two-hour cycle bookended by defrosts



The final heat pump cycle plot shows one of the longer heat pump cycles for RTU2F with a duration of about 14 hours. The RTU appeared to be able to modulate capacity to match the heating load quite well at these ambient conditions of roughly 47°F.

Figure 25. RTU2F 14-hour heat pump cycle



Supplemental Gas Use

Supplemental gas heating was rarely observed on RTU3F, and it never occurred on RTU2F during heating season. As noted in the results, the supplemental gas use appeared to be uncorrelated to the outdoor air temperature and did not provide a significant share of the heating capacity. RTU3F not only used gas heat, but also sometimes used gas heat in conjunction with the heat pump in both heating and cooling or defrost modes.

Gas Heat and Heat Pump Heat + Gas Heat

The following plots highlight operation that was labelled as gas heat mode, but heat pump heat + gas heat is also evident in every plot except the December 2023 example. In some cases, there are a few gas heat cycles followed by heat pump heating. In other cases, the gas heat cycles follow compressor heating. In addition, it was common to see operation transition from gas heat to heat pump heat + gas heat or vice versa, as the gas would remain on as the compressor started or the gas would turn on before the compressor stopped. This behavior occurred over a wide range of ambient temperatures, with the example from October 2023 occurring at about 55°F and the example from January 2024 taking place below 30°F.

Figure 26. RTI3F gas heat cycles transitioning to heat pump heat + gas heat then heat pump heat

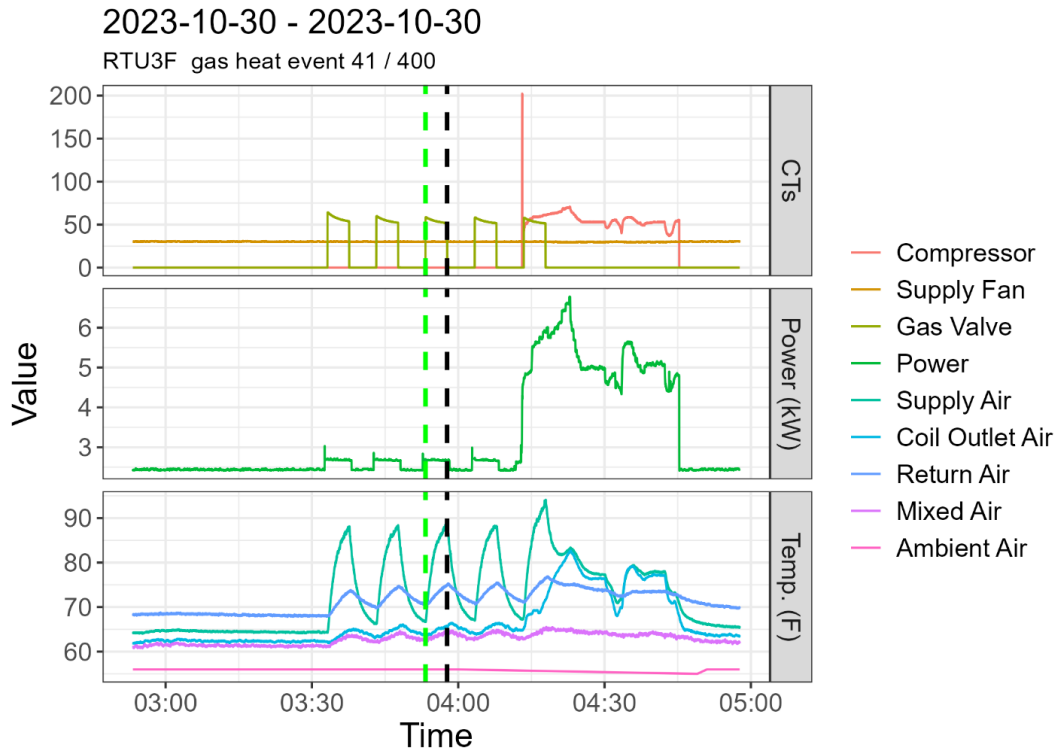


Figure 27. RTU3F heat pump heat followed by heat pump heat + gas heat then gas heating cycles

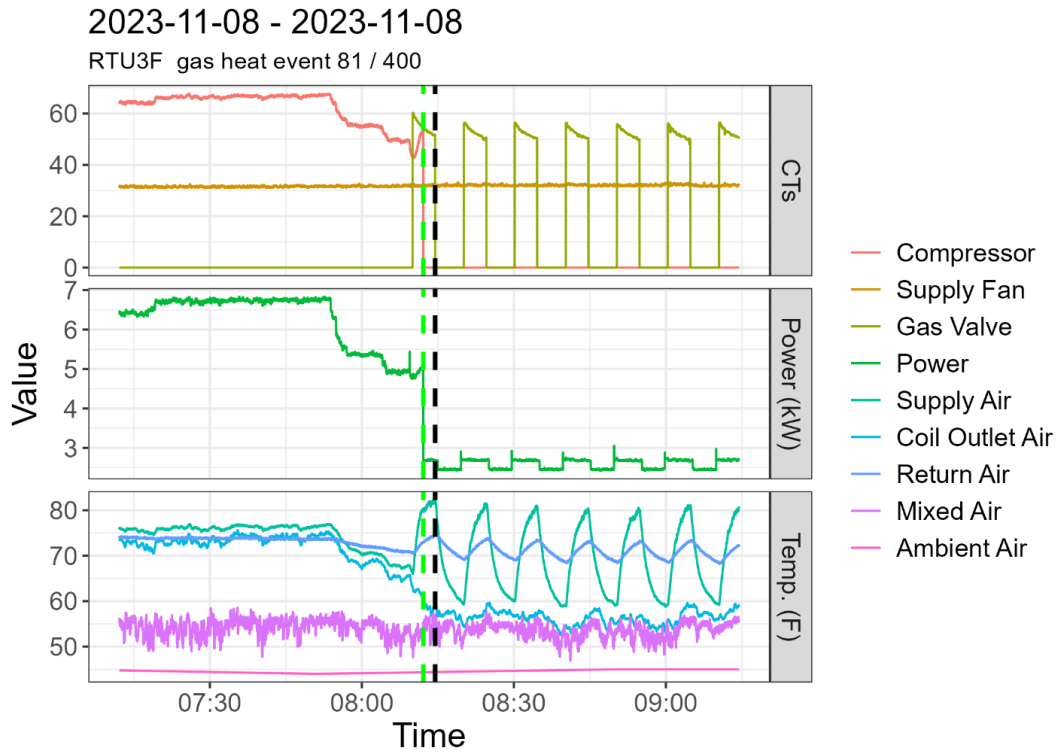


Figure 28. RTU3F standalone gas heat cycles

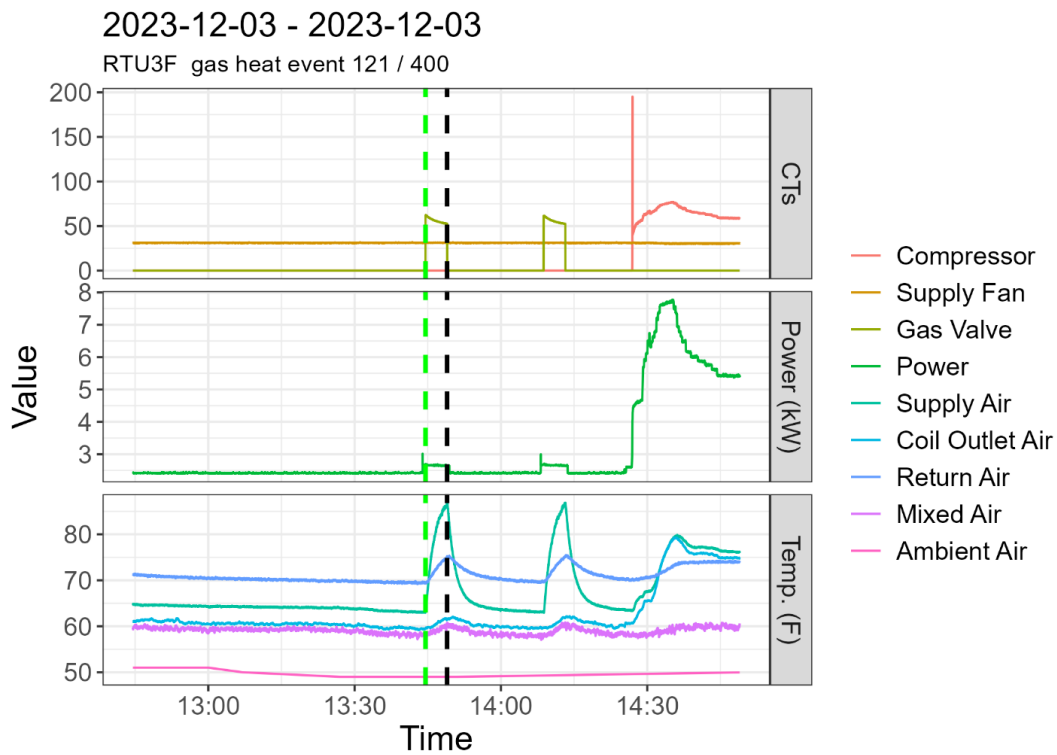


Figure 29. RTU3F gas heat cycles followed by HP heat + gas heat at lower ambient temperature

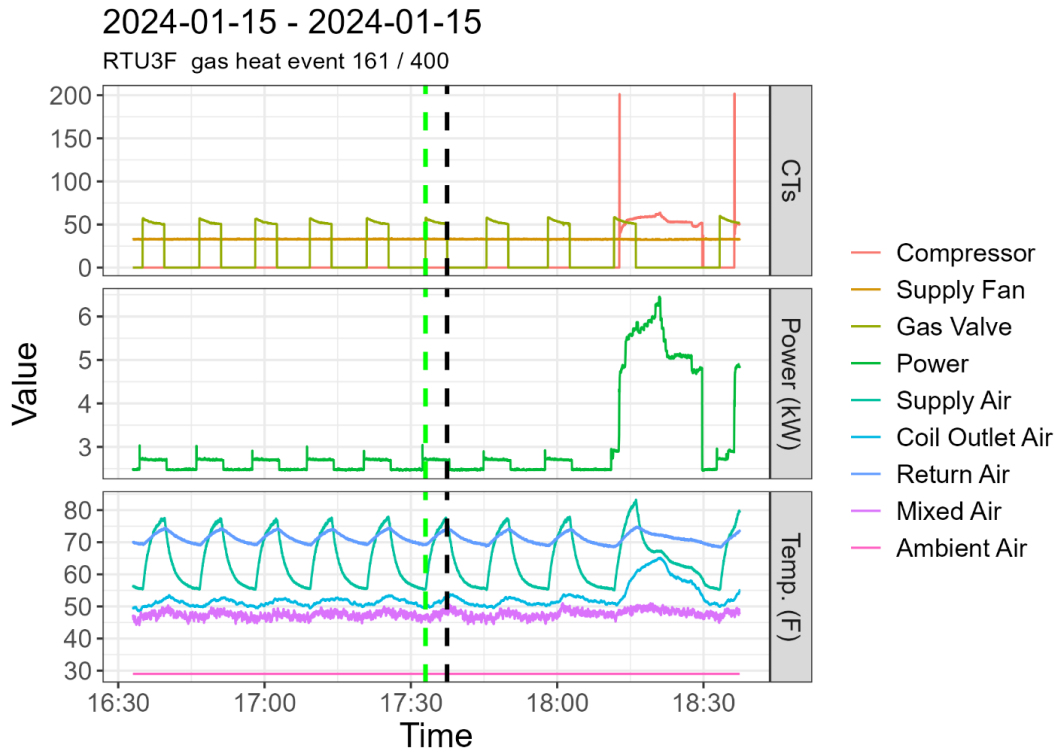
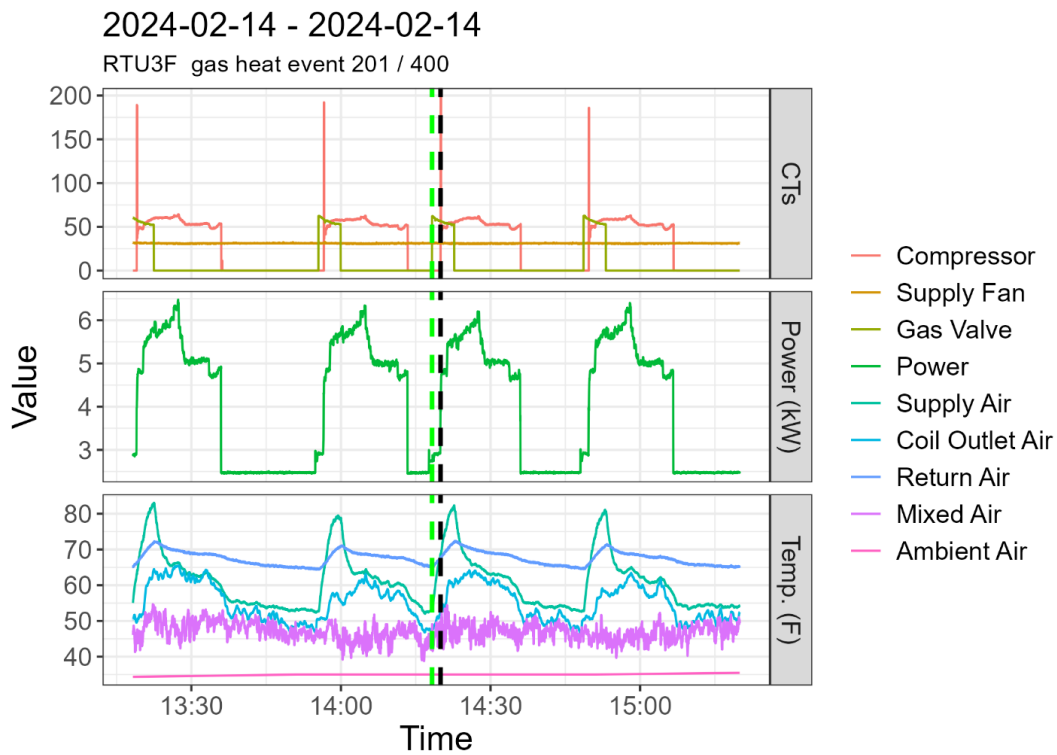


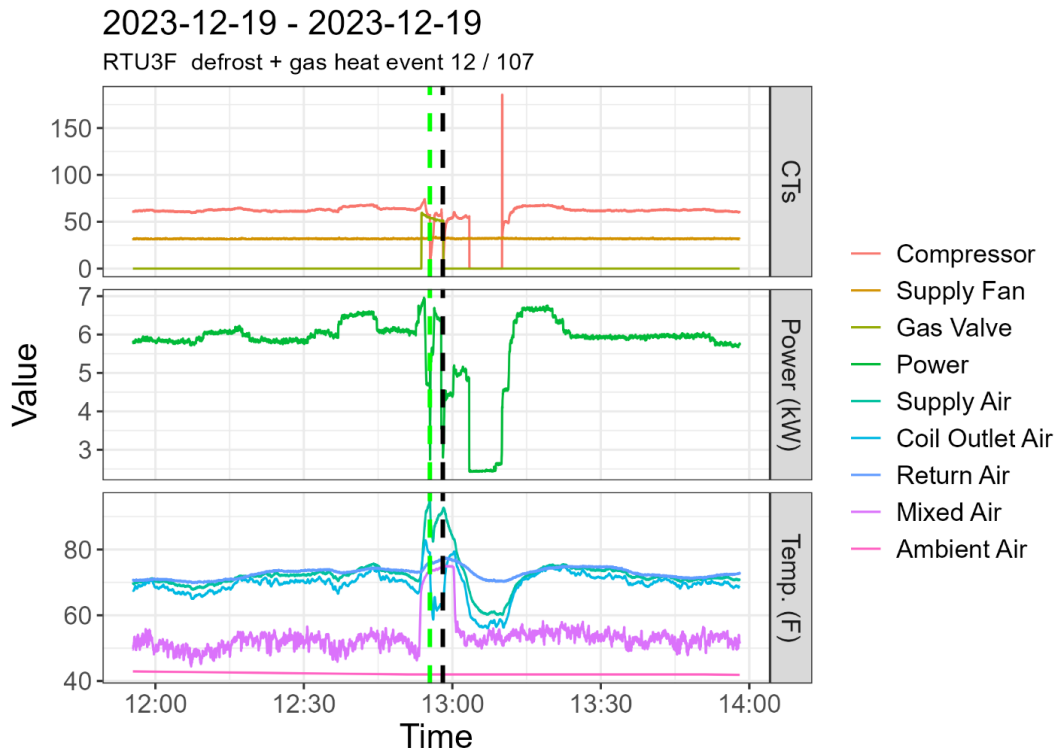
Figure 30. RTU3F each gas heat cycles transitions to heat pump heat + gas heat



Defrost + Gas Heat

There were 107 examples of an unexpected operating condition in which RTU3F was in defrost mode while using supplemental gas heat. Each of the examples reviewed appeared to be due to a defrost occurring while supplemental gas heat was active, or supplemental gas heat turning on during a defrost. The example shown in Figure 31 begins in heat pump heating, then transitions to heat pump heat + gas heat. When a defrost occurred, the mode was labeled as defrost + gas heat because the gas was active. When the defrost cycle ended, the gas also turned off, so the operating mode changed back to heat pump heating.

Figure 31. RTU3F typical defrost + gas heat event



Supplemental Gas Use Explanation

There was no gas use on RTU2F because the adjustable parameter **SuplHtg Hi OAT Lk** was configured to 0°F instead of its default value of 55°F. **SuplHtg Hi OAT Lk** is defined in OM 1141-6 as follows:

SuplHtg Hi OAT Lk is an adjustable item that sets a high outdoor ambient temperature value above which supplemental heating is locked out

This parameter was still set to the default value of 55°F on RTU3F. While gas use was allowed at temperatures less than 55°F on RTU3F, it did not seem necessary for space temperature control when it was used and was probably being activated for minimum discharge air temperature control. In this mode, it is possible to activate an internal control algorithm designed to protect the compressor from operating with a low differential pressure. The parameter **EffHtgOATLk** is related to this control. It is a status-only item that varies, and when it is lower than the ambient temperature, the compressor is prevented from operating. This parameter and related parameters are defined as follows in the operating manual OM 1141-6.

EffHtgOATLk is a status-only item that displays the current value that is being used for high outdoor ambient compressor heating lock out. Normally this value reads the same as the **Htg Hi OAT Lk** but can be lower due to the low differential pressure limiting function while the unit is operating in the Heating or MinDAT states.

Htg Hi OAT Lk is an adjustable item that sets a high outdoor ambient temperature value above which compressor heating is locked out.

During a site visit, the supplemental heat audibly turned on in an RTU that is not monitored as part of the project. While the gas heat was active on this unit, the **EffHtgOATLk** value was observed to be less than the ambient temperature. After the gas heat terminated, the **EffHtgOATLk** value changed to 100°F, matching the **Htg Hi OAT Lk** as described in the manual.

Figure 32. Controller on RTU2F FRONT (not monitored) showing Eff Htg Hi OAT Lk < Htg Hi OAT Lk



This control sequence explains why the system occasionally used gas at moderate ambient temperatures, but it does not explain why the system was able to enter heat pump heat + gas heat or defrost + gas heat modes.

Minimum discharge air temperature control is believed to be the mode that causes the system to operate in heat pump heat + gas heat and defrost + gas heat modes. There is some conflicting information in the operating manual regarding the behavior of the minimum discharge air temperature (MinDAT) control. On page 129, the manual states in the section **Heat Pump Control, Rebel Units 3 to 15 Ton**:

If compressor heating is available it is used first to provide the heating source during the MinDAT and Heating states. If compressor heating is unavailable (as during defrost operation for example) or inadequate to meet the heating requirements during these states, supplemental heating will be used to add to or in lieu of the compressor heating.

However, in an earlier section of the Operator's Guide (p. 99), Min DAT is described as follows:

If heating is enabled and there is no heating load (normally FanOnly operating state), the controller activates the units heating equipment as required to prevent the discharge air temperature from becoming too cool if the Min DAT Control Flag is set to yes via the Heating menu (Commission Unit/

Heating/MinDAT Ctrl). Only back up gas, electric or hot water is used. Heat Pump operation is not used because the required cycling at low head pressure may over stress the compressor oil management system.

Based on observations of RTU3F, the first definition of MinDAT operation applies in this case.

ACKNOWLEDGEMENTS

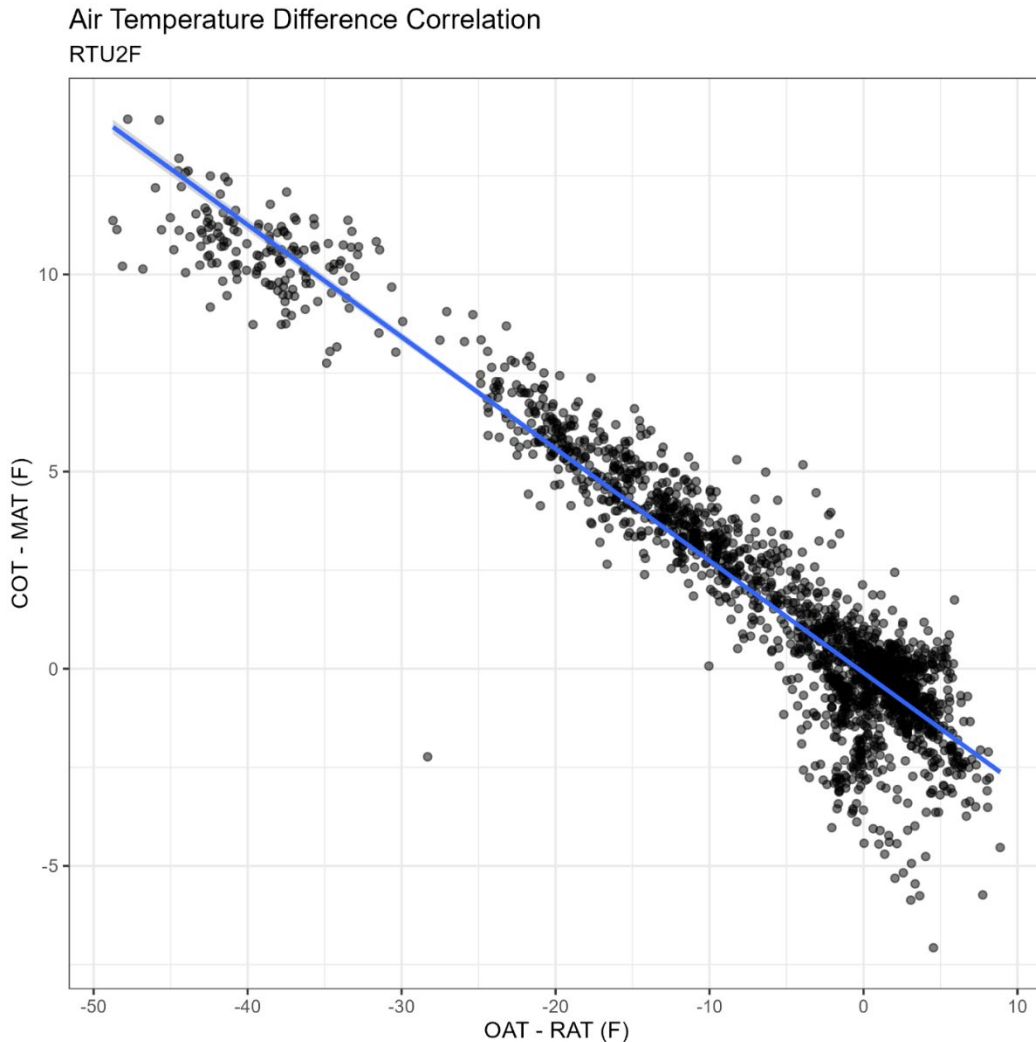
Center for Energy and Environment would like to express their sincere gratitude to those who have supported us throughout this research. Special thanks to Daikin Comfort Technologies and Daikin Applied Americas for their insightful feedback and assistance with coordinating this project. Specifically, we would like to thank Vince Fuentesz, Ryohei Hinokuma, Eric Joseph, and Will Ward for all their assistance.

APPENDIX: MIXED AIR TEMPERATURE CORRECTION

The mixed air temperature was adjusted in data post-processing to correct for bias toward the outdoor air temperature that was resulting in unrealistically high COPs.

The adjustment was based on the assumption that in fan-only mode, the temperature difference across the heat pump coil (i.e., the coil delta T) should be zero. However, the measured coil delta T appeared to be a linear function of the outside and return temperature difference.

Figure 33. Linear Correlation of original COT – MAT to OAT – RAT in fan-only mode



Mixed air temperature is nominally a weighted average of the RAT and OAT with weighting based on the outside air fraction, but due to instrumentation limitations, it tended to be biased toward the OAT in this application. The coil outlet sensor was assumed to be accurate due to higher air velocity and more upstream air mixing. Linear regression was used to find the relationship between measured coil delta T and the OAT-RAT temperature difference. Then, the following equations were used to correct the measured MAT values to their estimated “true” values.

$$\begin{aligned}(COT - MAT)_{true} &= 0 \\ (COT - MAT)_{meas} &= \beta_1(OAT - RAT) + \beta_0 \\ (COT - MAT)_{meas} - (COT - MAT)_{true} &= \beta_1(OAT - RAT) + \beta_0 - 0\end{aligned}$$

Assuming that $COT_{true} = COT_{meas}$ gives the transformation:

$$MAT_{true} = MAT_{meas} + \beta_1(OAT - RAT) + \beta_0$$

After applying the transformation, the regression line for $COT - MAT$ vs. $OAT - RAT$ in fan-only mode fell along the x-axis ($COT - MAT = 0$) as expected.

Figure 34. Linear Correlation of transformed COT - MAT to OAT - RAT in fan-only mode

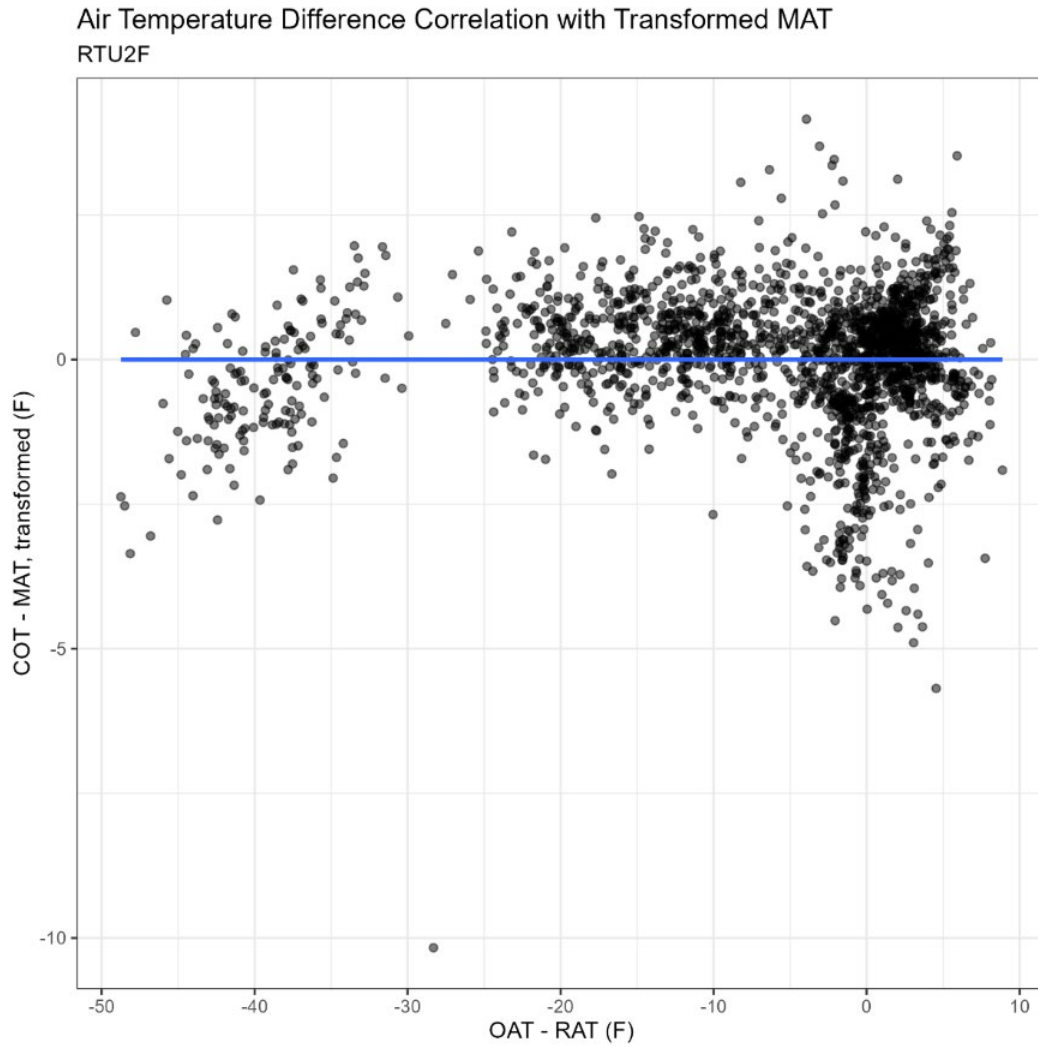
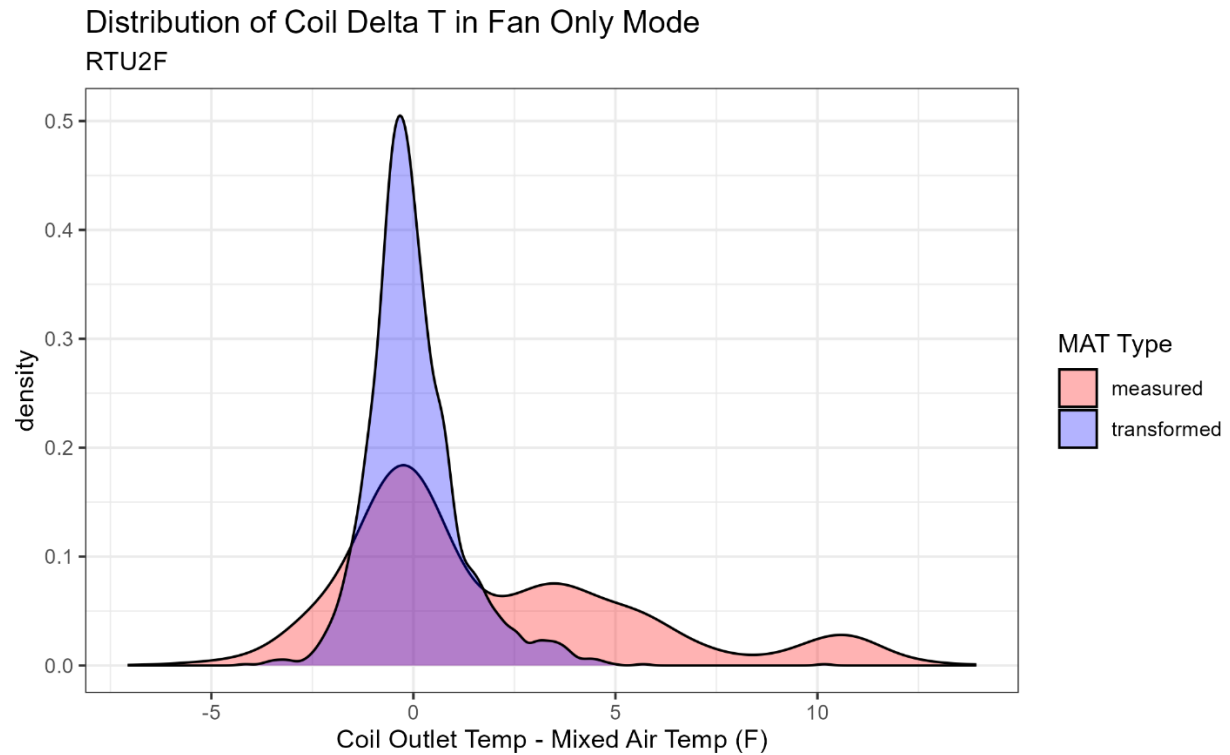
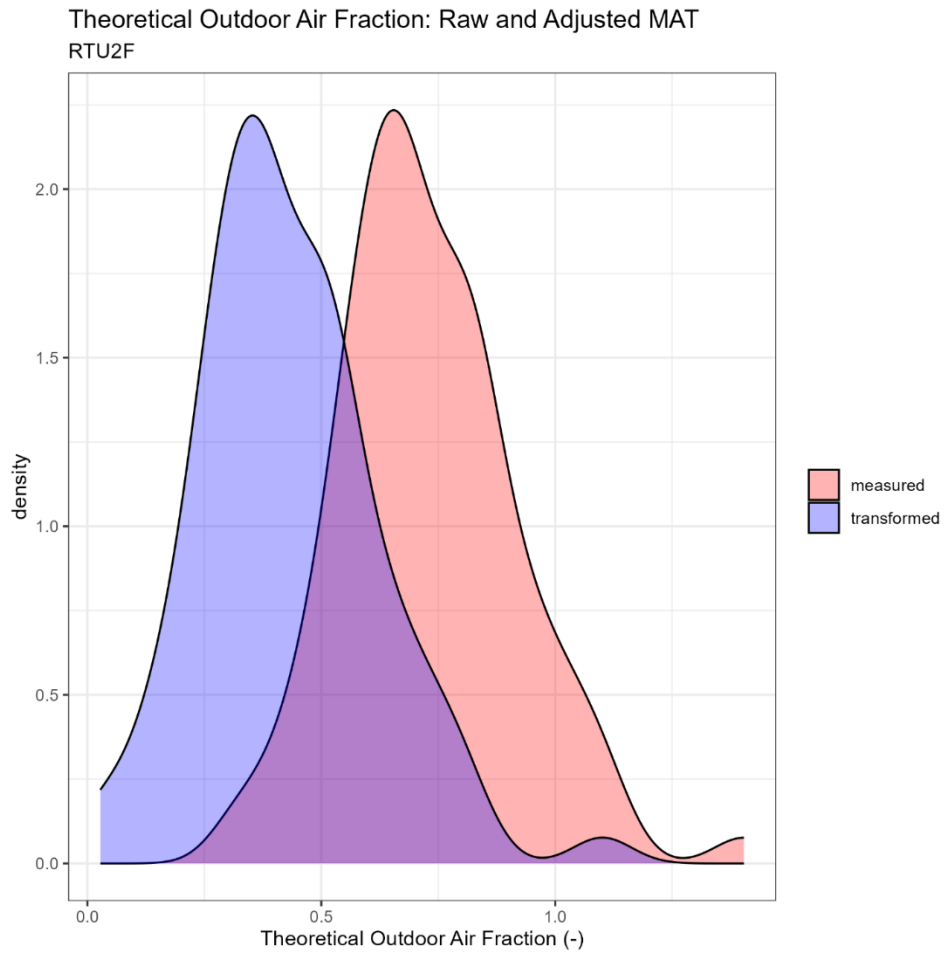


Figure 35. Distributions of coil outlet minus mixed air temperatures

Support for adjusting the MAT came from the estimated outdoor air fraction plots, which showed the distributions of theoretical outdoor air fraction for the same periods of fan-only operation calculated with both the raw and adjusted MAT values. For both RTUs, the theoretical outdoor air fraction distribution shifted to be centered about 0.3 or 0.4, which is much closer to the expected value of 0.3 for the outdoor air fraction.

Figure 36. Verification of MAT adjustment



REFERENCES

Daikin Applied. 2023. *Operation and Maintenance Manual: MicroTech Unit Controller for Rebel Commercial Packaged Rooftop Systems*. Minneapolis, Minnesota: Daikin Applied.

New York City. 2024. *LL97 Greenhouse Gas Emissions Reduction*. Accessed December 16, 2024. <https://www.nyc.gov/site/buildings/codes/ll97-greenhouse-gas-emissions-reductions.page>.

U.S. EPA. 2024. *Emission Factors for Greenhouse Gas Inventories*. Accessed October 11, 2024. <https://www.epa.gov/system/files/documents/2024-02/ghg-emission-factors-hub-2024.pdf>.